Chapter I

ATOMS, NUCLEI, AND ENERGY

Introduction

IN PRINCIPLE, the distribution of the elements among coexisting phases in equilibrium can be predicted, if one knows the Gibbs free energies of formation and activity coefficients of all chemical species in all phases as functions of temperature, pressure, and compositions of phases. Because this is not always possible, many geochemists attempt to explain and predict the geochemical behavior of various elements by their atomic properties, such as electron configuration, ionization energies, ionic radii, ionic potentials, electric polarizability, crystal lattice energies, hydrolysis constants, solubility products, and electronegativity. This kind of approach has proved to be useful but has also caused confusion when the exact physical meaning of those parameters is ignored.

In order to provide a framework for the discussion in the following chapters, these atomic properties and their closely interrelated nature are reviewed in the following sections. For ease of explaining the observed relative abundance of nuclides in the solar nebula in the next chapter, some pertinent nuclear properties are also reviewed here.

I-1. Periodic Table of the Elements and Electron Configurations of Atoms

An atom consists of a nucleus containing protons and neutrons, with electrons orbiting around the nucleus. In an electrically neutral atom, the number of electrons is equal to the number of protons. The number of protons in the nucleus of an atom is called the **atomic number** (Z). There are 112 known chemical elements so far, as shown in the periodic table (Table I-1a). Elements with atomic numbers between 104 and 112 are artificial radionuclides with short half-lives. The names and symbols for these elements are still contested (Table I-1b). The periodic table consists of seven horizontal rows or periods. The vertical columns under the arabic numerals with A and B are called groups of chemical elements. Elements in the same group are called **congeners** and have similar physicochemical properties. Therefore, the periodic law states that the physicochemical properties of the elements change in periodic or repeated cycles as their atomic numbers increase. For example,

TABLE I-1A

Periodic table

Period	Group																	
	1	2	3	4	5	6	7	8	9	10	11	12	13	14	15	16	17	18
	1A	2A	3B	4B	5B	6B	7B	8B			1B	2B	3A	4A	5A	6A	7A	8A
	s-block		d-block										p-block					
1	1 H																	2 He
2	3 Li	4 Be											5 B	6 C	7 N	8 O	9 F	10 Ne
3	11 Na	12 Mg											13 Al	14 Si	15 P	16 S	17 Cl	18 Ar
4	19 K	20 Ca	21 Sc	22 Ti	23 V	24 Cr	25 Mn	26 Fe	27 Co	28 Ni	29 Cu	30 Zn	31 Ga	32 Ge	33 As	34 Se	35 Br	36 Kr
5	37 Rb	38 Sr	39 Y	40 Zr	41 Nb	42 Mo	43 Tc	44 Ru	45 Rh	46 Pd	47 Ag	48 Cd	49 In	50 Sn	51 Sb	52 Te	53 I	54 Xe
6	55 Cs	56 Ba	*57 La	72 Hf	73 Ta	74 W	75 Re	76 Os	77 Ir	78 Pt	79 Au	80 Hg	81 Tl	82 Pb	83 Bi	84 Po	85 At	86 Rn
7	87 Fr	88 Ra	#89 Ac	104 Rf	105 Db	106 Sg	107 Bh	108 Hs	109 Mt	110	111	112						

Lanthanides	*57 La	58 Ce	59 Pr	60 Nd	61 Pm	62 Sm	63 Eu	64 Gd	65 Tb	66 Dy	67 Ho	68 Er	69 Tm	70 Yb	71 Lu	
Actinides	#89 Ac	90 Th	91 Pa	92 U	93 Np	94 Pu	95 Am	96 Cm	97 Bk	98 Cf	99 Es	100 Fm	101 Md	102 No	103 Lr	
	f-block															

TABLE I-1B
Some atomic properties of the elements

Z	*Symbol*	*Name*	*Atomic weight*	*Electron configuration*	*Oxidation states*	*Density (g/cm^3)*	*Melting point (K)*	*Boiling point (K)*
1	H	Hydrogen	1.00794	$1s^1$	1	(0.0899)	14.0	20.28
2	He	Helium	4.00260	$1s^2$		(0.1785)	0.95	4.216
3	Li	Lithium	6.941	$1s^2 2s^1$	1	0.53	453.7	1615
4	Be	Beryllium	9.01218	$1s^2 2s^2$	2	1.85	1560	2757
5	B	Boron	10.81	$1s^2 2s^2 p^1$	3	2.34	2365	4275
6	C	Carbon	12.011	$1s^2 2s^2 p^2$	2, ±**4**	2.26	3825	5100
7	N	Nitrogen	14.0067	$1s^2 2s^2 p^3$	2, ±**3**, 4, 5	(1.251)	63.15	77.35
8	O	Oxygen	15.9994	$1s^2 2s^2 p^4$	−2	(1.429)	54.8	90.18
9	F	Flourine	18.9984	$1s^2 2s^2 p^5$	−1	(1.696)	53.5	85
10	Ne	Neon	20.1797	$1s^2 2s^2 p^6$		(0.90)	24.55	27.1
11	Na	Sodium	22.98977	$[Ne]3s^1$	1	0.97	371.0	1156
12	Mg	Magnesium	24.305	$[Ne]3s^2$	2	1.74	922	1380
13	Al	Aluminum	26.98154	$[Ne]3s^2 p^1$	3	2.70	933.5	2740
14	Si	Silicon	28.0855	$[Ne]3s^2 p^2$	4	2.33	1683	3522
15	P	Phosphorus	30.97376	$[Ne]3s^2 p^3$	±3, 4, **5**	1.82	317.3	553
16	S	Sulfur	32.066	$[Ne]3s^2 p^4$	±2, 4, **6**	2.70	392.2	717.8
17	Cl	Chlorine	35.4527	$[Ne]3s^2 p^5$	±**1**, 3, 5, 7	(3.214)	172.2	239.1
18	Ar	Argon	39.948	$[Ne]3s^2 p^6$		(1.784)	83.9	87.4
19	K	Potassium	39.0983	$[Ar]4s^1$	1	0.86	336.8	1033
20	Ca	Calcium	40.078	$[Ar]4s^2$	2	1.55	1112	1757
21	Sc	Scandium	44.9559	$[Ar]3d^1 4s^2$	3	2.99	1814	3109
22	Ti	Titanium	47.88	$[Ar]3d^2 4s^2$	3,**4**	4.54	1945	3560
23	V	Vanadium	50.9415	$[Ar]3d^3 4s^2$	2,3,4,**5**	6.11	2163	3650
24	Cr	Chromium	51.996	$[Ar]3d^5 4s^1$	2, **3**, 6	7.19	2130	2945

TABLE I-1B *Continued*

Z	*Symbol*	*Name*	*Atomic weight*	*Electron configuration*	*Oxidation states*	*Density (g/cm^3)*	*Melting point (K)*	*Boiling point (K)*
25	Mn	Manganese	54.9380	$[Ar]3d^5 4s^2$	**2**, 3, 4, 6, 7	7.44	1518	2335
26	Fe	Iron	55.847	$[Ar]3d^6 4s^2$	2, **3**	7.874	1808	3135
27	Co	Cobalt	58.9332	$[Ar]3d^7 4s^2$	**2**, 3	8.90	1768	3143
28	Ni	Nickel	58.6934	$[Ar]3d^8 4s^2$	**2**, 3	8.90	1726	3187
29	Cu	Copper	63.546	$[Ar]3d^{10} 4s^1$	1, **2**	8.96	1357	2840
30	Zn	Zinc	65.39	$[Ar]3d^{10} 4s^2$	2	7.13	692.7	1180
31	Ga	Gallium	69.723	$[Ar]3d^{10} 4s^2 p^1$	3	5.91	302.9	2478
32	Ge	Germanium	72.61	$[Ar]3d^{10} 4s^2 p^2$	4	5.32	1211	3107
33	As	Arsenic	74.9216	$[Ar]3d^{10} 4s^2 p^3$	±**3**, 5	5.78	1090	876
34	Se	Selenium	78.96	$[Ar]3d^{10} \mathbf{4}s^2 p^4$	−2, **4**, 6	4.79	494	958
35	Br	Bromine	74.904	$[Ar]3d^{10} 4s^2 p^5$	±**1**, 5	3.12	265.9	332
36	Kr	Krypton	83.80	$[Ar]3d^{10} 4s^2 p^6$		(3.75)	116	120
37	Rb	Rubidium	85.4678	$[Kr]5s^1$	1	1.532	312.6	961
38	Sr	Strontium	87.62	$[Kr]5s^2$	2	2.54	1042	1655
39	Y	Yttrium	88.9059	$[Kr]4d^1 5s^2$	3	4.47	1795	3611
40	Zr	Zirconium	91.224	$[Kr]4d^2 5s^2$	4	6.51	2128	4682
41	Nb	Niobium	92.9064	$[Kr]4d^4 5s^1$	3, **5**	8.57	2742	5015
42	Mo	Molybdenum	95.94	$[Kr]4d^5 5s^1$	2, 3, 4, 5, **6**	10.22	2896	4912
43	Tc*	Technetium	98	$[Kr]4d^5 5s^2$	7	11.5	2477	4538
44	Ru	Ruthenium	101.07	$[Kr]4d^7 5s^1$	2, **3**, **4**, 6, 8	12.37	2523	4425
45	Rh	Rhodium	102.9055	$[Kr]4d^8 5s^1$	2, **3**, 4	12.41	2236	3970
46	Pd	Palladium	106.42	$[Kr]4d^{10} 5s^0$	**2**, 4	12.0	1825	3240
47	Ag	Silver	107.868	$[Kr]4d^{10} 5s^1$	1	10.5	1235	2436
48	Cd	Cadmium	112.41	$[Kr]4d^{10} 5s^2$	2	8.65	594.2	1040

49	In	Indium	114.82	$[Kr]4d^{10}5s^2p^1$	3	7.31	429.7	2350
50	Sn	Tin	118.71	$[Kr]4d^{10}5s^2p^2$	2, **4**	7.31	505.1	2876
51	Sb	Antimony	121.757	$[Kr]4d^{10}5s^2p^3$	±**3**, 5	6.69	904	1860
52	Te	Tellurium	127.60	$[Kr]4d^{10}5s^2p^4$	−2, **4**, 6	6.24	722.7	1261
53	I	Iodine	126.9045	$[Kr]4d^{10}5s^2p^5$	±**1**, 5, 7	4.93	386.7	457.5
54	Xe	Xenon	131.29	$[Kr]4d^{10}5s^2p^6$		(5.90)	161.4	165.1
55	Cs	Cesium	132.9054	$[Xe]6s^1$	1	1.87	301.5	944
56	Ba	Barium	137.33	$[Xe]6s^2$	2	3.59	1002	2078
57	La	Lanthanum	138.9055	$[Xe]5d^16s^2$	3	6.15	1193	3737
58	Ce	Cerium	140.12	$[Xe]4f^15d^16s^2$	**3**, 4	6.77	1071	3715
59	Pr	Praseodymium	140.9077	$[Xe]4f^36s^2$	**3**, 4	6.77	1204	3785
60	Nd	Neodymium	144.24	$[Xe]4f^46s^2$	3	7.01	1294	3347
61	Pm*	Promethium	145	$[Xe]4f^56s^2$	3	7.22	1315	3273
62	Sm	Samarium	150.36	$[Xe]4f^66s^2$	2, **3**	7.52	1345	2064
63	Eu	Europium	151.965	$[Xe]4f^76s^2$	2, **3**	5.24	1090	1870
64	Gd	Gadolinium	157.25	$[Xe]4f^86s^2$	3	7.9	1585	3539
65	Tb	Terbium	158.9253	$[Xe]4f^96s^2$	**3**, 4	8.23	1630	3496
66	Dy	Dysprosium	162.50	$[Xe]4f^{10}6s^2$	3	8.55	1682	2835
67	Ho	Holmium	164.9303	$[Xe]4f^{11}6s^2$	3	8.80	1743	2968
68	Er	Erbium	167.26	$[Xe]4f^{12}6s^2$	3	9.07	1795	3136
69	Tm	Thulium	168.9342	$[Xe]4f^{13}6s^2$	2, **3**	9.32	1818	2220
70	Yb	Ytterbium	173.04	$[Xe]4f^{14}6s^2$	2, **3**	6.97	1097	1467
71	Lu	Lutetium	174.967	$[Xe]4f^{14}5d^16s^2$	3	9.84	1936	3668
72	Hf	Hafnium	178.49	$[Xe]4f^{14}5d^26s^2$	4	13.31	2504	4875

TABLE I-1B *Continued*

Z	*Symbol*	*Name*	*Atomic weight*	*Electron configuration*	*Oxidation states*	*Density (g/cm^3)*	*Melting point (K)*	*Boiling point (K)*
73	Ta	Tantalum	180.9479	$[Xe]4f^{14}5d^36s^2$	5	16.65	3293	5730
74	W	Tungsten	183.85	$[Xe]4f^{14}5d^46s^2$	2, 3, 4, 5, **6**	19.3	3680	5828
75	Re	Rhenium	186.207	$[Xe]4f^{14}5d^56s^2$	−1, 2, 4, 6, **7**	21.0	3455	5870
76	Os	Osmium	190.2	$[Xe]4f^{14}5d^66s^2$	2, 3, **4**, 6, 8	22.6	3300	5300
77	Ir	Iridium	192.22	$[Xe]4f^{14}5d^76s^2$	2, 3, **4**, 6	22.6	2720	4700
78	Pt	Platinum	195.08	$[Xe]4f^{14}5d^96s^1$	2, **4**	21.45	2042	4100
79	Au	Gold	196.9665	$[Xe]4f^{14}5d^{10}6s^1$	1, **3**	18.88	1337	3130
80	Hg	Mercury	200.59	$[Xe]4f^{14}5d^{10}6s^2$	1, **2**	13.55	234.3	630
81	Tl	Thallium	204.383	$[Xe]4f^{14}5d^{10}6s^2p^1$	**1**, 3	11.85	577	1746
82	Pb	Lead	207.2	$[Xe]4f^{14}5d^{10}6s^2p^2$	**2**, 4	11.35	600.6	2023
83	Bi	Bismuth	208.9804	$[Xe]4f^{14}5d^{10}6s^2p^3$	**3**, 5	9.75	544.5	1837
84	Po	Polonium	209	$[Xe]4f^{14}5d^{10}6s^2p^4$	2, **4**	9.3	527	1235
85	At	Astatine	210	$[Xe]4f^{14}5d^{10}6s^2p^5$	±**1**, 3, 5, 7		575	610
86	Rn	Radon	222	$[Xe]4f^{14}5d^{10}6s^2p^6$		(9.73)	202	211
87	Fr	Francium	223	$[Rn]7s^1$	1		300	950
88	Ra	Radium	226.0254	$[Rn]7s^2$	2	5	973	1900
89	Ac	Actinium	227.0278	$[Rn]6d^17s^2$	3	10.07	1324	3470
90	Th	Thorium	232.0381	$[Rn]6d^27s^2$	4	11.72	2028	5061
91	Pa	Protactinium	231.0359	$[Rn]5f^26d^17s^2$	4, **5**	15.4	1845	4300
92	U	Uranium	238.029	$[Rn]5f^36d^17s^2$	3, 4, 5, **6**	18.95	1408	4407
93	Np*	Neptunium	237.0482	$[Rn]5f^46d^17s^2$	3, 4, **5**, 6	20.2	912	4175
94	Pu*	Plutonium	224	$[Rn]5f^67s^2$	3, **4**, 5, 6	19.84	913	3505
95	Am*	Americium	243	$[Rn]5f^77s^2$	**3**, 4, 5, 6	13.7	1449	2880
96	Cm*	Curium	247	$[Rn]5f^76d^17s^2$	3	13.5	1620	

97	Bk*	Berkelium	247	[Rn]5$f^{9}7s^{2}$	**3**, 4	
98	Cf*	Californium	251	[Rn]5$f^{10}7s^{2}$	3	1170
99	Es*	Einsteinium	252	[Rn]5$f^{11}7s^{2}$		1130
100	Fm*	Fermium	257	[Rn]5$f^{12}7s^{2}$		1800
101	Md*	Mendelevium	258	[Rn]5$f^{13}7s^{2}$		1100
102	No*	Nobelium	259	[Rn]5$f^{14}7s^{2}$		1100
103	Lr*	Lawrencium	260	[Rn]5$f^{14}6d^{1}7s^{2}$		1900
104	Rf*	Rutherfordium	261	[Rn]5$f^{14}6d^{2}7s^{2}$		
105	Db*	Dubnium	262	[Rn]5$f^{14}6d^{3}7s^{2}$		
106	Sg*	Seaborgium	263	[Rn]5$f^{14}6d^{4}7s^{2}$		
107	Bh*	Bohrium	262	[Rn]5$f^{14}6d^{5}7s^{2}$		
108	Hs*	Hassium	265	[Rn]5$f^{14}6d^{6}7s^{2}$		
109	Mt*	Meitnerium	266	[Rn]5$f^{14}6d^{7}7s^{2}$		
110	Uun*	Ununnilium	269	[Rn]5$f^{14}6d^{9}7s^{1}$		
111	Uun*	Unununium	272	[Rn]5$f^{14}6d^{10}7s^{1}$		
112	Uub*	Ununbium	277	[Rn]5$f^{14}6d^{10}7s^{2}$		

Notes: Density is at 300 K and one atmosphere, except that those in parentheses, which are in the gaseous state, are in units of g/ℓ. The bold numbers are the most common oxidation states for a given element. Elements with asterisks are artificial radionuclides.

the molar atomic volume of the elements (= atomic weight/density) at 25°C and 1 atmosphere changes periodically as a function of the atomic number (Figure I-1). For some elements that are in the gaseous state at 25°C and 1 atmosphere pressure, the density in the liquid state at the melting point is used.

The similarity in physicochemical properties among certain elements is often a reflection of their similar **electron configurations**. According to quantum mechanics, the energy levels (or states) and most probable spatial distribution of electrons in the orbital cloud around an atomic nucleus can be described by four **quantum numbers**, i.e., n (principal), l (angular momentum), m_l (magnetic), and m_s (spin). For the physical meaning of the four quantum numbers, one should refer to any standard physical chemistry textbook. According to the Pauli exclusion principle, no two electrons in an atom can have the same four quantum numbers.

The **principal quantum number**, n, is a positive integer that ranges from 1 to 7 for the known atoms in the ground (i.e., lowest-energy) state. The principal energy levels or states with $n = 1$ to 7 are often denoted as the K, L, M, N, O, P, and Q shells, respectively. For a given n, the **angular momentum quantum numbers**, l, are positive integers from 0 to $n - 1$. For example, if $n = 4$ then $l = 0, 1, 2, 3$. The energy levels with $l = 0, 1, 2, 3, 4$ are designated as the s, p, d, f, and g subshells, respectively.

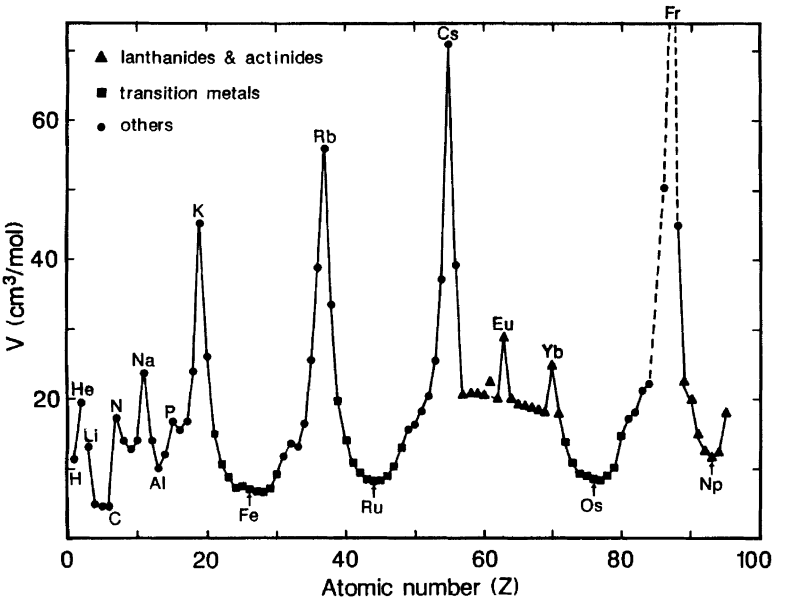

FIGURE I-1. Periodicity of molar volumes of elements at 25°C (except those for H, N, O, F, Cl, and noble gases are at or below their boiling points) and 1 atmosphere.

The combinations of n and l can define all the major subshells in atoms. For example, $nl = 1s; 2s, 2p; 3s, 3p, 3d; 4s, 4p, 4d, 4f; 5s, 5p, 5d, 5f, 5g$, etc. The relative energy levels of these subshells for neutral atoms in the ground state are schematically shown in Figure I-2 (from the lowest $1s$ to the highest $6d$; notice that the g subshell is unnecessary for accommodating electrons of atoms in the ground state). One should be aware that the relative energy levels of subshells are slightly different from those of Figure I-2 when the atoms are positively charged (i.e., cations). This point will be discussed later.

For a given l value, the **magnetic quantum number**, m_l, can have all integers between $-l$ and l including 0 (e.g., $l = 3$, $m_l = -3, -2, -1, 0, 1, 2, 3$). Thus, there are $(2l + 1)$ values of m_l for a given l. In addition, **the spin quantum number**, m_s, can have only two values (i.e., $+1/2$ and $-1/2$). Therefore, the combination of m_l and m_s produces $2(2l + 1)$ numbers of distinctive

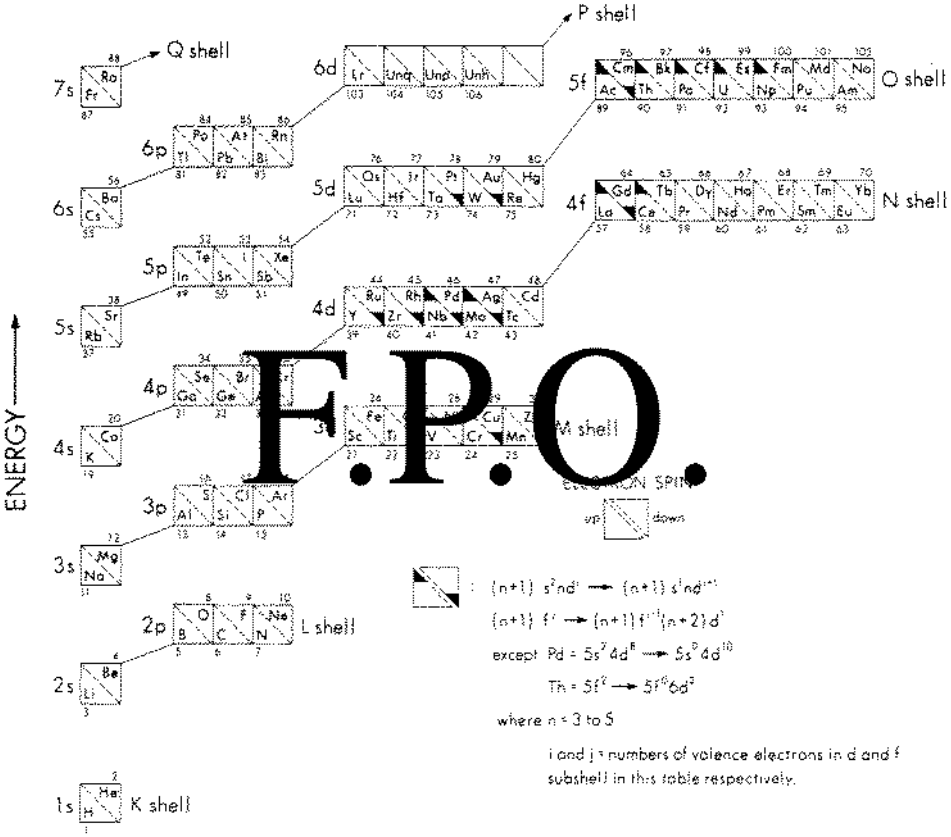

FIGURE I-2. Energy levels of subshells and the electron configurations of neutral elements. The exceptions to the given configuration are indicated by solid triangles.

quantum states of electrons with the same energy level, i.e., $2(2l + 1)$-fold energy degeneracy. In other words, the s subshell ($l = 0$) consists of one orbital; the p subshell ($l = 1$) has 3 orbitals; the d subshell ($l = 2$) has 5 orbitals; and the f subshell ($l = 3$) has 7 orbitals with the same energy levels. Each orbital can accommodate one pair of electrons spinning in opposite directions, schematically shown in Figure I-2 as cubic boxes with up and down triangles. The electron configuration of any atom with atomic number Z is constructed by feeding electrons one by one into the lowest empty orbitals of subshells until a number of electrons equal to the atomic number Z are all accommodated. The orbitals in the p, d, and f subshells should each be first filled by a single electron with parallel spin before electrons with opposite spins can enter any of those orbitals. For example, the electron configuration of Mn ($Z = 25$) is [Ar]$3d^5 4s^2$, where the superscripts represent the numbers of electrons in subshells and [Ar] the electron configuration equivalent to the Ar atom. $3d^5$ represents 5 electrons in the $3d$ subshell, and these 5 electrons are spinning in the same direction (parallel spins), each in one orbital. There are, however, many exceptions in Figure I-2: the energy levels of $(n + 1)s$ and $(n - 1)f$ are usually slightly lower than those of nd for most of the elements in Figure I-2, but the reverse is the case for some atoms (indicated by solid triangles). In this case, one or two electrons from the $(n + 1)s$ and $(n - 1)f$ subshells should move into the nd subshell. For example, the electron configurations of Cu ($Z = 29$) and Ce ($Z = 58$) are [Ar]$3d^9 4s^2$ and [Xe]$4f^2 6s^2$ according to Figure I-2 but in fact should be [Ar]$3d^{10} 4s^1$ and [Xe]$4f^1 5d^1 6s^2$, respectively.

The outermost two or three subshells are usually called the subshells of valence electrons. By convention, the subshells of the valence electrons are listed in increasing order of the principal quantum number as shown in Table I-1b (not in order of the subshell energy levels for the neutral atoms as shown in Figure I-2). The advantage of this convention is that the sequence of subshells of valence electrons is listed exactly in the increasing order of energy levels for cations. Therefore, one can easily obtain the electron configuration for any cation, M^{+z}, by simply taking away z electrons from the outermost subshell(s) of the neutral atom as given in Table I-1b.

The heavy zigzag line in Table I-1a separates the elements into **metals** on the left and **nonmetals** on the right. The elements bordering the zigzag line, such as B, Si, Ge, As, Sb, Te, and Po, are called **metalloids**. The characteristic properties of all metals are high electric and thermal conductivity, high reflectivity (metallic luster), mechanical ductility, and malleability, and their power to replace hydrogen in acids. The elements can also be classified into four blocks according to which subshell is filled by the last valence electron. They are the *s*-**block** of the alkali (group 1A) and alkaline earth metals (group 2A), the *d*-**block** of the transition metals (group 1B to 8B),

the f-**block** of the lanthanides and actinides, and the p-**block** of group 3A to 8A as shown in Table I-1a and Figure I-2.

I-2. Atomic Nuclei and Nuclear Binding Energies

The total number of protons Z and neutrons N in an atomic nucleus is called the **mass number** $A(= Z + N)$ of the nucleus. Nuclei with identical Z but different N are called **isotopes**, whereas nuclei with identical N but different Z are called **isotones**. Nuclei with identical A but variable N and Z are **isobars**. By convention, an atomic nucleus is represented by a chemical symbol with its mass number A as a left-hand side superscript and its atomic number Z as a left-hand side subscript, e.g., ${}^{16}_{8}\mathrm{O}$ and ${}^{12}_{6}\mathrm{C}$. Since the elemental symbol already implies the atomic number, the subscript of the atomic number is often omitted, e.g., ${}^{16}\mathrm{O}$ and ${}^{12}\mathrm{C}$.

There are about 268 stable nuclei in nature: 159 nuclei with even Z and even N; 55 with even Z and odd N; 49 with odd Z and even N; and only 5 with odd Z and odd N combinations (i.e., ${}^{2}_{1}\mathrm{H}$, ${}^{6}_{3}\mathrm{Li}$, ${}^{10}_{5}\mathrm{B}$, ${}^{14}_{7}\mathrm{N}$, and ${}^{50}_{23}\mathrm{V}$). It is apparent that nuclei with paired protons and/or paired neutrons are favored among stable nuclei. Figure I-3 also shows that nuclei with even Z (or even N) usually have more than three stable isotopes (or isotones), and nuclei with odd Z (or odd N) usually have only one isotope (or isotone), or occasionally two. Nuclei with odd A (i.e., even Z–odd N or odd Z–even N) have only one stable isobar, while nuclei with even A (i.e., even Z–even N, except for the five odd Z–odd N nuclei mentioned earlier) have one to three stable isobars. The neutron to proton ratio (N/Z) is about one for stable nuclei with Z (or N) less than 20, but increases gradually with increasing Z and reaches about 1.5 for the heaviest stable nucleus ${}^{209}_{83}\mathrm{Bi}$ (Figure I-3). Any nucleus with Z and N values falling outside the stable nuclei field in Figure I-3 is unstable, and will undergo various radioactive decay steps (such as α and β decays and spontaneous fission) so that the N/Z ratio will eventually approach one of those stable nuclei.

According to international convention, the mass of one mole of ${}^{12}\mathrm{C}$ atoms ($= 6.022045 \times 10^{23}$ atoms = Avogadro's number) equals 12 grams, and the mass of one ${}^{12}\mathrm{C}$ atom is defined to equal 12 **atomic mass units** (amu). Therefore one atomic mass unit (amu) is equivalent to $1/(6.022045 \times 10^{23}) = 1.66056 \times 10^{-24}$ g. Its energy equivalent is 1.492442×10^{-3} erg = 931.5023 MeV (1 MeV $= 10^6$ electronvolts). Accordingly, the rest mass of one hydrogen atom M_H (one proton plus one electron) is 1.007825037 amu = 938.79134 MeV; the rest mass of a neutron M_n = 1.008665012 amu = 939.57378 MeV; and the rest mass of an electron M_e = 0.00054858026 amu = 0.5110034 MeV. The masses of various neutral atoms are summarized by Bievre et al. (1984).

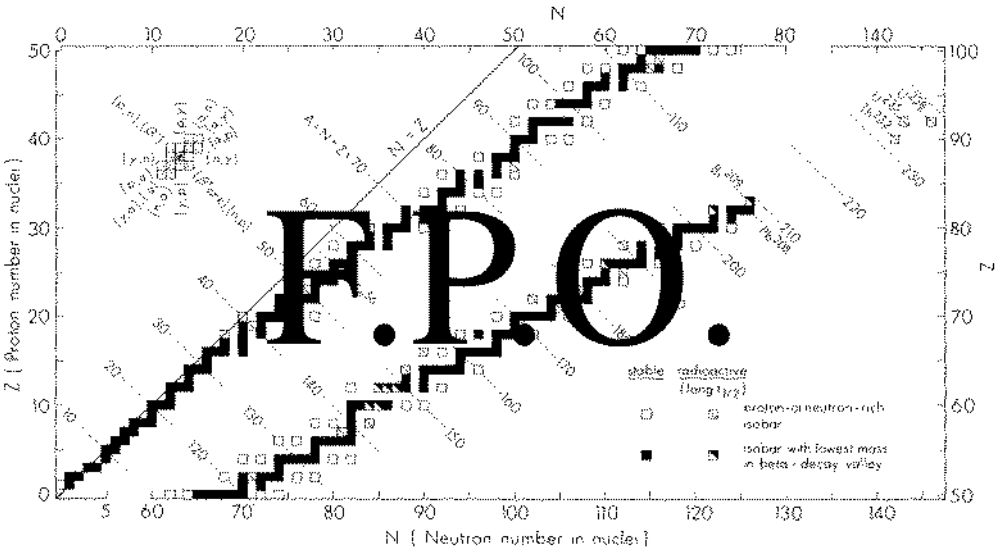

FIGURE I-3. Known stable nuclei and long-half-life radionuclides on the Z-N plane. Notice that the diagram is split into two at $Z = 50$ and $N = 60$.

The energy released in the formation of a nucleus from its component nucleons (i.e., hydrogen atoms and neutrons) is called the **binding energy of the nucleus**, Q_b, i.e.,

$$Z \cdot M_{\mathrm{H}} + N \cdot M_n \rightarrow {}^{A}_{Z}M + Q_b, \text{ i.e., } Q_b = Z \cdot M_{\mathrm{H}} + N \cdot M_n - {}^{A}_{Z}M. \quad \text{(I-1)}$$

For example, the binding energy of the ${}^{4}_{2}$He nucleus is

$$\begin{aligned} Q_b = 2M_{\mathrm{H}} + 2M_n - {}^{4}\mathrm{He} &= 2 \times 1.0078250 + 2 \times 1.0086650 \\ &\quad - 4.0026033\,\text{amu} \\ &= 0.030376\,\text{amu} = 28.2960\,\text{MeV}. \end{aligned}$$

The relative stability of nuclei can be represented by the binding energy per nucleon (Q_b/A). Figure I-4 shows the Q_b/A values calculated from equation I-1 as a function of A for all stable nuclei and for some heavy radioactive nuclei ($A > 226$). The complete listing of Q_b/A values is given by Yoshihara et al. (1985). The Q_b/A values generally increase with increasing A up to a broad maximum around $A = 56$, which corresponds to the ^{56}Fe nucleus, then decrease gradually. Therefore ^{56}Fe is the most stable of all nuclei. Energetically it is possible to release nuclear energies (exothermic process) by fusing more than two lighter nuclei ($A < 56$) to form a new nucleus with a higher Q_b/A value (fusion process). For example,

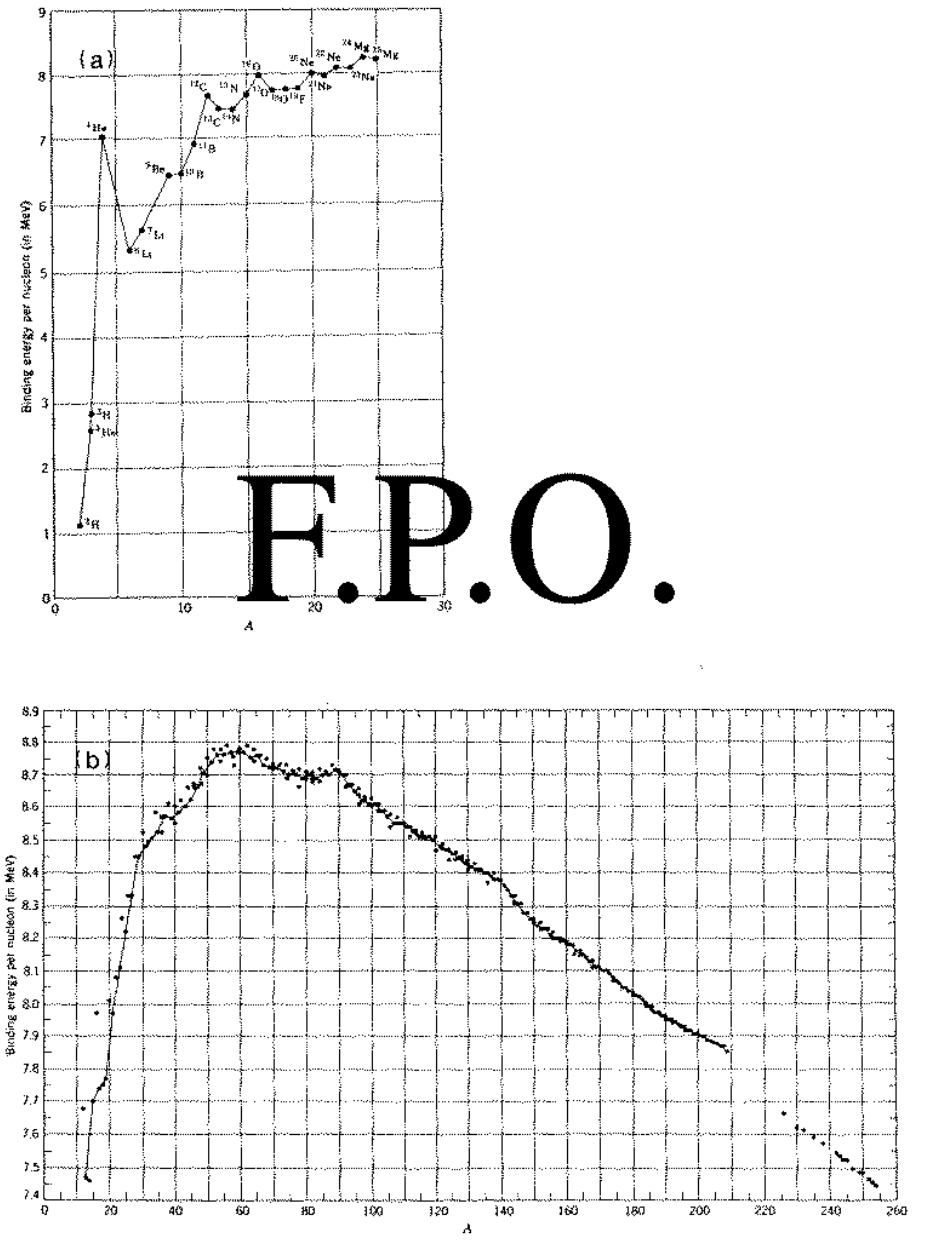

FIGURE I-4. Binding energy per nucleon as a function of mass number A for nuclei between (a) $2 \leq A \leq 25$ and (b) $12 \leq A \leq 250$ (the solid line connects the odd-A nuclei). The highest point in the broad maximum is ^{56}Fe. Reprinted by permission of John Wiley & Sons Inc.

$^{4}_{2}\mathrm{He} + {}^{12}_{6}\mathrm{C} \rightarrow {}^{16}_{8}\mathrm{O} + Q(\text{energy released});$

$$\begin{aligned} Q &= {}^{4}_{2}\mathrm{He} + {}^{12}_{6}\mathrm{C} - {}^{16}_{8}\mathrm{O} \\ &= 4.00260 + 12 - 15.99491 \\ &= 0.00769\,\text{amu} = 7.16\,\text{MeV}. \end{aligned} \tag{I-2a}$$

For nuclei with $A > 56$, the only way to release the nuclear energy is to split a nucleus into lighter nuclei with higher Q_b/A values (fission process). For example,

$$\begin{aligned} &{}^{235}_{92}\mathrm{U} + n \rightarrow {}^{140}_{56}\mathrm{Ba} + {}^{93}_{36}\mathrm{Kr} + 3n + Q; \\ &Q = 174\,\text{MeV}. \end{aligned} \tag{I-2b}$$

In Figure I-4, the Q_b/A values for $^{4}_{2}\mathrm{He}$, $^{12}_{6}\mathrm{C}$, $^{16}_{8}\mathrm{O}$, $^{20}_{10}\mathrm{Ne}$, and $^{24}_{12}\mathrm{Mg}$ are higher than those of their immediate neighbors. In other words, the nuclei that are multiples of the helium nucleus have extra stability. This extra stability can be seen clearly in the theoretical minimum energy required to remove one neutron,

$$Q_n \left(= {}^{A-1}_{Z}M + M_n - {}^{A}_{Z}M\right), \tag{I-2c}$$

or one proton,

$$Q_p \left(= {}^{A-1}_{Z-1}M + M_{\mathrm{H}} - {}^{A}_{Z}M\right), \tag{I-2d}$$

from a nucleus as shown in Figure I-5 for Q_n.

Analogous to the ions with noble gas electron configuration are the nuclei with neutron or proton numbers of 2, 8, 20, 28, 50, 82, and 126, which also have extra stability. Those numbers are called **magic numbers**. Nuclei with N and/or $Z = 8$, 50, 82, and 126 also have very low capture cross sections for thermal neutrons (Friedlander et al., 1981).

For a set of isobars, the term $(Z \cdot M_{\mathrm{H}} + N \cdot M_n)$ in equation I-1 is near constant; therefore the lower the mass of the isobar, ${}^{A}_{Z}M$, the higher is Q_b, i.e., the isobar with minimum nuclear mass is the most stable. For example, the mass of a set of isobars with odd mass number ($A = 135$) can be represented by a parabolic function of Z (Figure I-6 left). The stable nucleus ^{135}Ba lies at the bottom of the parabola. The isobars on the neutron-rich side of the parabola (left arm) are unstable and will be transformed into ^{135}Ba by successive negative β decays (${}^{A}_{Z}M \rightarrow {}^{A}_{Z+1}M^{+} + e^{-} + \bar{\nu}$, where $\bar{\nu}$ is the antineutrino and e^{-} is the electron). The isobars on the proton-rich side of the parabola (right arm) will again be transformed into ^{135}Ba by successive positive β decays (${}^{A}_{Z}M \rightarrow {}^{A}_{Z-1}M^{-} + e^{+} + \nu$, where ν is the neutrino and e^{+} is

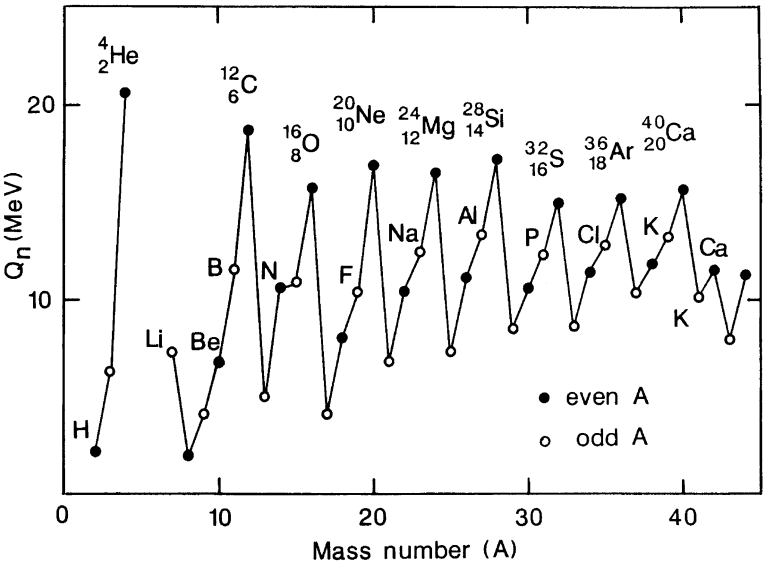

FIGURE I-5. Separation energy of a neutron (Q_n) from nuclei ($1 \leq A \leq 44$). Notice the peaks for the multiple-α-particle nuclei.

the positron) or by electron capture (${}^{A}_{Z}M + e^{-} \rightarrow {}^{A}_{Z-1}M + \nu$), i.e., a nucleus captures an electron from the inner electron orbitals of the atom. Therefore this kind of parabola is often called the β-**stability valley**.

In the case of isobars with even A (= 136, Figure I-6 right), the mass of the isobars can be represented by two parabolas (the upper one for odd Z–odd N and the lower one for even Z–even N). There are two metastable nuclei, ^{136}Xe and ^{136}Ce, in addition to the most stable ^{136}Ba. In principle, ^{136}Xe and ^{136}Ce, can decay into ^{136}Ba by a so-called double β decay process (i.e., simultaneous emission of two $e^{\pm}$ particles or capture of two electrons). However, the probability of a double β decay is extremely low. Metastable nuclei such as ^{136}Xe and ^{136}Ce are also often called the **shielding** nuclei (open squares in Figure I-3), whereas the stable ^{136}Ba is called the **shielded** nucleus. The shielding nuclei preclude the formation of the shielded nucleus by way of successive β decay of neutron- or proton-rich unstable isobars.

Nuclear reactions such as that in equation I-2a can be expressed by the short-hand notation ^{12}C$(\alpha, \gamma)^{16}$O; i.e., the lighter reacting particle and the lighter resulting particle are written within parentheses between the heavier initial and final nuclei and separated by a comma. For a spontaneous decay reaction, there is often no light reacting particle, thus it is omitted in the notation. For example, $^{3}\mathrm{H} \rightarrow {}^{3}\mathrm{He} + e^{-} + \bar{\nu}$ is written as $^{3}\mathrm{H}(e^{-}\bar{\nu})^{3}\mathrm{He}$. A

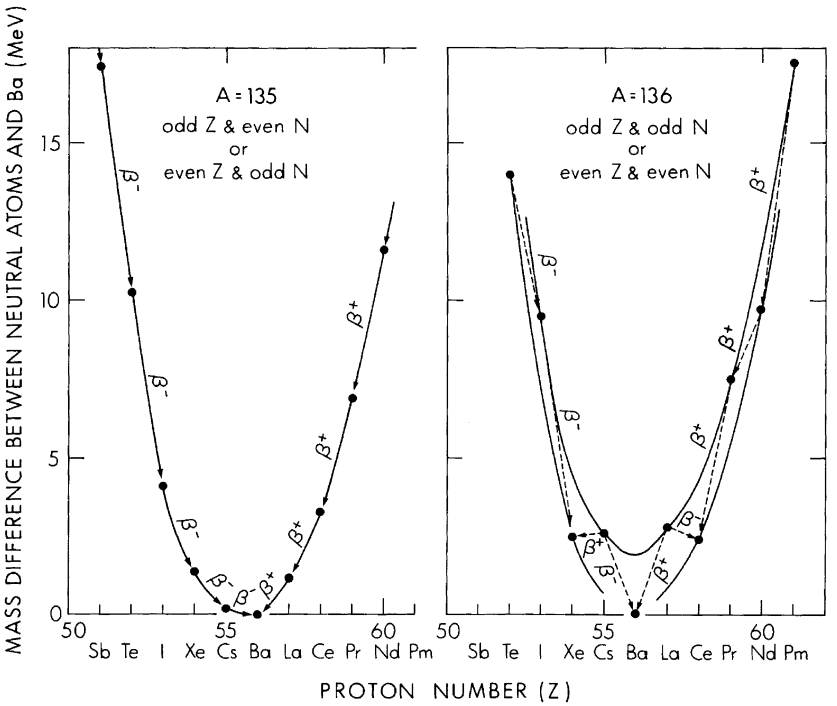

FIGURE I-6. Beta-stability-valley diagrams for isobars $A = 135$ (left) and $A = 136$ (right). The β symbols and arrows indicate consecutive beta decays.

spontaneous electron capture reaction such as $^{23}\mathrm{Mg} + e^- \rightarrow {}^{23}\mathrm{Na} + \nu$ can be expressed as $^{23}\mathrm{Mg}(e^-, \nu)^{23}\mathrm{Na}$. A consecutive reaction

$$^{12}\mathrm{C} + {}^{4}\mathrm{He} \rightarrow {}^{16}\mathrm{O} + \gamma$$
$$^{16}\mathrm{O} + {}^{4}\mathrm{He} \rightarrow {}^{20}\mathrm{Ne} + \gamma$$

can be simplified as

$$^{12}\mathrm{C}(\alpha, \gamma)^{16}\mathrm{O}(\alpha, \gamma)^{20}\mathrm{Ne}.$$

The isotopic ratios of an element in natural samples are usually compared to those of a chosen standard material. For example, **standard mean ocean water**, abbreviated as SMOW (Craig, 1961), is the standard material for oxygen and hydrogen isotopes. The deviation of oxygen and hydrogen iso-

topic ratios of any sample from those of SMOW is given by the following convenient notations:

$$\delta^{18}\mathrm{O} = \left[\frac{(^{18}\mathrm{O}/^{16}\mathrm{O})_{\text{sample}}}{(^{18}\mathrm{O}/^{16}\mathrm{O})_{\text{SMOW}}} - 1\right] \times 1000‰,$$

$$\delta^{17}\mathrm{O} = \left[\frac{(^{17}\mathrm{O}/^{16}\mathrm{O})_{\text{sample}}}{(^{17}\mathrm{O}/^{16}\mathrm{O})_{\text{SMOW}}} - 1\right] \times 1000‰,$$

$$\delta\mathrm{D} = \left[\frac{(\mathrm{D}/\mathrm{H})_{\text{sample}}}{(\mathrm{D}/\mathrm{H})_{\text{SMOW}}} - 1\right] \times 1000‰,$$

where D is deuterium (^{2}H). A δ^{18}O value of $+8‰$ for basaltic rock means that the sample is 8 per mil (‰) enriched in ^{18}O relative to SMOW. The absolute oxygen and hydrogen isotopic ratios of SMOW are

$$^{18}\mathrm{O}/^{16}\mathrm{O} = 200520 \pm 45 \times 10^{-8} \qquad \text{(Baertschi, 1976)},$$

$$^{17}\mathrm{O}/^{16}\mathrm{O} = 38309 \pm 34 \times 10^{-8} \qquad \text{(McKeegan, 1987)},$$

$$\mathrm{D}/\mathrm{H} = 15576 \pm 5 \times 10^{-8} \qquad \text{(Hagemann et al., 1970)}.$$

If two coexisting phases A and B are isotopically in equilibrium, the ratio of ^{18}O/^{16}O in phase A to the ratio in phase B is called the **fractionation factor** ($\alpha_{\mathrm{A/B}}$), i.e.,

$$\alpha_{\mathrm{A/B}} = \frac{(^{18}\mathrm{O}/^{16}\mathrm{O})_A}{(^{18}\mathrm{O}/^{16}\mathrm{O})_B}.$$

For example, $\alpha_{\text{water/vapor}} = 1.0092$ at 25°C. This means that the water phase is enriched in ^{18}O relative to the vapor phase. The $\alpha_{\mathrm{A/B}}$ can be related to δ_{A} and δ_{B} by

$$\alpha_{\mathrm{A/B}} = \frac{\delta_A/1000 + 1}{\delta_B/1000 + 1}$$

or approximated by $10^3 \ln \alpha_{\mathrm{A/B}} \approx \delta_{\mathrm{A}} - \delta_{\mathrm{B}}$.

I-3. Cohesive Energies among the Atoms of Pure Metals and Nonmetals

The atoms of a pure solid metal are held together mainly by the so-called **metallic bonds**, which can be visualized as resulting from the attraction between a network of metal cations and the "sea" of freely mobile electrons (mainly valence electrons). The atoms or polyatomic molecules of nonmetals in solid state are held together mainly by the **weak Van der Waals force**.

The weak Van der Waals force results from the interaction of the instantaneous electric dipole moments of nonmetal atoms. The electrons of an atom may have their center of charge coincident with that of a nucleus at one instant (thus no electric dipole moment), but at another instant it may lie beside the nucleus, thus forming an instantaneous electric dipole moment (two opposite but equal charges multiplied by distance). Rather than pointing in random fashion, the vectors of the instantaneous electric dipole moments of the neighboring atoms are more often synchronized (due to dipole-induced dipoles), thus resulting in a weak net attraction (London, 1930).

The magnitude of the cohesive energy holding the atoms or polyatomic molecules of the pure solid elements together can be best represented by the **enthalpy of sublimation**, ΔH^0_{sbl}, which is the energy required to convert one mole of atoms or polyatomic molecules from solid to gas at the standard state (25°C and 1 atmosphere). For elements that are gas or liquid at the standard state, the ΔH^0_{sbl} values at their melting points are adopted. The periodicity of ΔH^0_{sbl} as a function of atomic number is shown in Figure I-7 and listed

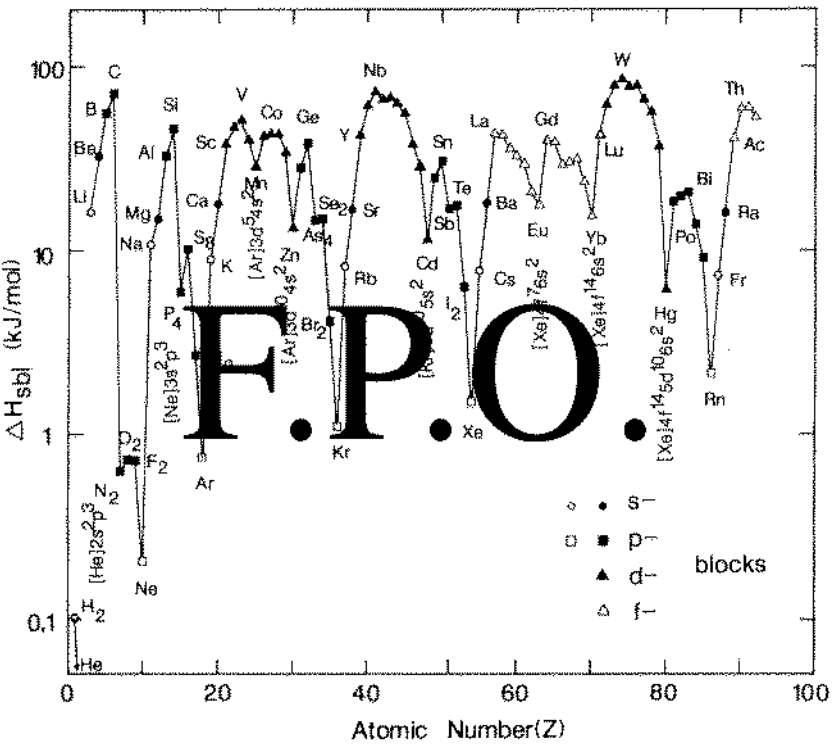

FIGURE I-7. Heats of sublimation $\left(\Delta H^0_{\text{sbl}}\right)$ of solid elements as a function of Z. The minima are always associated with full or half-full outermost subshells.

in Table I-2. The minima of ΔH^0_{sbl} are always associated with atoms that have full or half-full outermost subshells. The polyatomic molecules shown in Table I-2 and Figure I-7 represent the most stable gaseous species for those elements at the standard state.

TABLE I-2
Heats of sublimation (ΔH^0_{sbl}) and boiling points (T_b) of the elements

Z	ΔH^0_{sbl} *(kJ/mol)*	T_b (K)	Z	ΔH^0_{sbl} *(kJ/mol)*	T_b (K)	Z	ΔH^0_{sbl} *(kJ/mol)*	T_b (K)
H_2	*1.01	20.3	Ge	379.6	3107	Pm	293	3273
He	*0.13	4.2	As	302.5	876	Sm	206.7	2064
			As_4	144	876	Eu	175.3	1870
Li	159.4	1615	Se	227.1	958	Gd	397.5	3539
Be	324.3	2757	Se_2	146	958	Tb	388.7	3496
B	562.7	4275	Br_2	*41.1	332	Dy	290.4	2835
C	716.7	5100	Kr	*10.7	120	Ho	300.8	2968
N_2	*6.25	77.4				Er	317.1	3136
O_2	*7.26	90.2	Rb	80.9	961	Tm	232.2	2220
F_2	7.2	85	Sr	164.4	1655	Yb	152.3	1467
Ne	2.04	27.1	Y	421.3	3611	Lu	427.6	3668
			Zr	608.8	4682	Hf	619.2	4876
Na	107.3	1156	Nb	725.9	5015	Ta	782	5730
Mg	147.7	1380	Mo	658.1	4912	W	849.4	5828
Al	326.4	2740	Tc	678	4538	Re	769.9	5870
Si	455.6	3522	Ru	642.7	4425	Os	791	5300
P	314.6	553	Rh	556.9	3970	Ir	665.3	4701
P_4	58.9	553	Pd	378.2	3240	Pt	565.3	4100
S	278.8	717.8	Ag	284.6	2436	Au	366.1	3130
S_8	102.3	717.8	Cd	112	1040	Hg	61.3	630
Cl_2	*26.8	239.1	In	243.3	2346	Tl	182.2	1746
Ar	*7.5	87.3	Sn	302.1	2876	Pb	195	2023
			Sb	262.3	1860	Bi	207.1	1837
K	89.2	1033	Sb_2	167	1860	Po	146	1235
Ca	178.2	1757	Te	196.7	1261	At	90.4	610
Sc	377.8	3109	Te_2	172	1261	Rn	*21.3	211
Ti	469.9	3560	I	107.8	458			
V	514.2	3650	I_2	62.4	458	Fr	73	950
Cr	396.6	2945	Xe	*14.9	165	Ra	159	1900
Mn	280.7	2335				Ac	406	3470
Fe	416.3	3135	Cs	76.1	944	Th	598.3	5061
Co	424.7	3143	Ba	180	2078	Pa	607	4300
Ni	429.7	3187	La	431	3737	U	535.6	4407
Cu	338.3	2840	Ce	423	3715	Np		4175
Zn	130.7	1180	Pr	355.6	3785	Pu	352	3505
Ga	277	2478	Nd	327.6	3347	Am		2880

Notes: ΔH^0_{sbl} of elements with asterisks is estimated at the melting point, otherwise at 25°C. ΔH^0_{sbl} are mostly from Wagman et al. (1982) with some additional data from Dean (1985). The boiling point data are copied from Table I-1b.

Interestingly, the **boiling points** of the elements (Table I-2) are closely related to ΔH^0_{sbl} as shown in Figure I-8 (notice the different correlation lines for metals and nonmetals). Thus, the stronger the cohesive energy among the atoms of a pure element in the solid state, the higher is the boiling point of the element. Also, the boiling points and ΔH^0_{sbl} values for the *p*- and *s*-block elements are generally lower than those for the *d*- and *f*-block elements in the same period (Figure I-7).

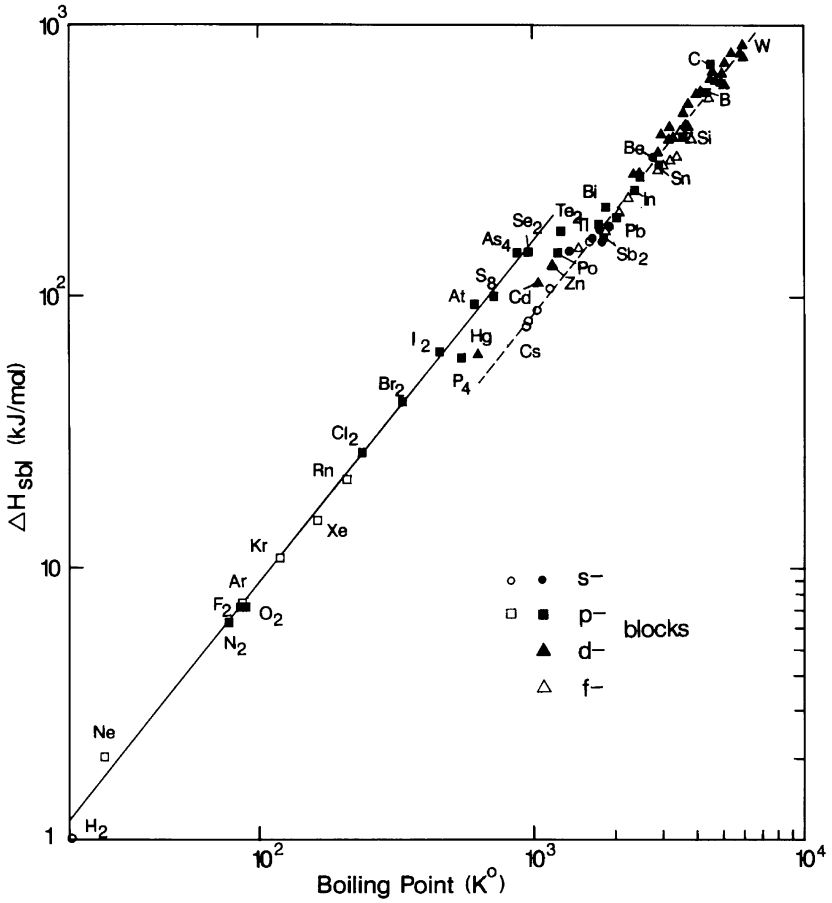

FIGURE I-8. The good correlation between the boiling point of elements and the heats of sublimation $\left(\Delta H^0_{sbl}\right)$ of atoms or polyatomic molecules of solid elements. Noble gases and polyatomic molecules (except Sb_2) fall on the same correlation line.

I-4. Ionization Energies and Electron Affinities of Gaseous Atoms and Ions

The energy required to remove the least strongly bound electron from a gaseous atom $M(\mathrm{g})$, to infinite distance is called the first **ionization energy** (or **ionization potential**) of the atom, I_1. The energies required to remove subsequent electrons are called the second (I_2), third (I_3), and up to zth (I_z) ionization energies, i.e.,

$$M(\mathrm{g}) + I_1 \rightarrow M^{+}(\mathrm{g}) + e^{-},$$

$$M(\mathrm{g}) + I_2 \rightarrow M^{+2}(\mathrm{g}) + e^{-},$$

$$\vdots$$

$$M^{z-1}(\mathrm{g}) + I_z \rightarrow M^{+z}(\mathrm{g}) + e^{-}.$$

The zth ionization energy, I_z, of $M^{z-1}(\mathrm{g})$ is equivalent to the binding energy of an electron to a gaseous cation $M^{+z}(\mathrm{g})$ in the reverse reaction above. Adding the above equations, one obtains

$$M(\mathrm{g}) + \Sigma I_z \rightarrow M^{+z}(\mathrm{g}) + ze^{-},$$

where ΣI_z is the **cumulative ionization energy** ($= I_1 + I_2 + \cdots + I_z$). Some gaseous neutral atoms can react spontaneously with an electron to form a monovalent gaseous anion, i.e.,

$$M(\mathrm{g}) + e^{-} \rightarrow M^{-1}(\mathrm{g}) + I_{-1}.$$

The energy released in the above equation (I_{-1}) is called the (first) **electron affinity** to a gaseous atom $M(\mathrm{g})$. The electron affinity is equivalent to the ionization energy of a monovalent anion. Similarly, we can define the cumulative electron affinity, ΣI_{-z}, as equal to the energy released in the spontaneous reaction

$$M(\mathrm{g}) + ze^{-} \rightarrow M^{-z}(\mathrm{g}) + \Sigma I_{-z}.$$

However, the data for ΣI_{-z} are scarce. By losing or gaining electrons, the neutral gaseous atoms can be transformed into various gaseous ions; but

the actual numbers of stable ions in chemical compounds are quite limited. According to their electron configuration, the most common stable ions can be classified into four main types: (1) **A-type cations and anions**, which have the electron configurations of noble gases; (2) **B-type cations** with the outermost subshell configuration of nd^{10}, $nd^{10}(n+1)s^2$, as well as [He]$2s^2$ and [Ne]$3s^2$; (3) the transition metal cations with the outermost d shells partially filled; and (4) the lanthanide and actinide cations with the outermost f subshells partially or totally filled.

The successive ionization energies I_1 up to I_7 (Dean, 1985) and I_{-1} (Bratsch, 1983; Hotop and Lineberger, 1985), for each element at 0 K are given in the Appendix Table A-1. The I_z and the **average binding energy**, $\Sigma I_z/z$, for common stable cations are summarized in Table I-3. The successive ionization energies at 298 K (25°C) can be obtained by adding 0.064 eV to each value in Appendix Table A-1 as explained in the footnote of the table. The ionization energy is also often expressed in terms of the ionization of one mole of gaseous atoms instead of a single atom. For example, 1 eV/atom = 96.5 kJ/mol = 23.1 kcal/mol.

The data for I_1 to I_4 are plotted as a function of atomic number (Z) in Figure I-9. The maxima are again always associated with the cations that have full or half-full outermost subshells. The minima are the cations with the outermost subshell configurations of ns^1 and np^1, i.e., the single electrons in the outermost s and p subshells are loosely held by the atoms. Figure I-9 also indicates that the energy levels of ns subshells are higher than those of $(n-1)d$ subshells for cations with identical valency, i.e., the $(n-1)d$ subshell is filled in by electrons prior to the ns subshell. The converse is the case for neutral atoms, as already shown in Figure I-2.

The successive ionization energies as a function of charge z for Ca (s-block); Cl, As, and Br (p-block); and Zn and Mn (d-block) are plotted in Figure I-10 (see page 27). Whenever an electron is taken away from a full or half-full subshell, there is always a break in the slope. For clarity and convenience hereafter, the ionization energy I_z will be considered only as the **electron binding energy** to gaseous cation M^{+z} unless noted otherwise. The plot of I_z against $\Sigma I_z/z$ for most common cations indicates a good linear relationship (Figure I-11, see page 27). Thus both parameters are interchangeable.

The I_z divided by the charge z is called the **polarizing power** of cation M^{+z} by Goldschmidt (1954). A nice periodicity of I_z/z as a function of atomic number Z is apparent in Figure I-12 (see page 28). The close relationship between I_z/z and the electronegativity will be discussed in Section I-7.

Application of the concept of the electron binding energy or ionization energy to many geochemical problems has been amply demonstrated by Ahrens (1952, 1953, 1954, 1983). In the following sections, its applications will be demonstrated wherever relevant.

TABLE I-3
Electron binding energy to cation $M^{+z}(I_z)$ and average electron binding energy ($\Sigma I_z/z$)

Z	z	I_z	$\Sigma I_z/z$	Z	z	I_z	$\Sigma I_z/z$	Z	z	I_z	$\Sigma I_z/z$
Ac-89	3	(19)	(12)	Hf-72	4	33.3	19.5		4	(41)	(24)
Ag-47	1	7.58	7.58	Hg-80	1	10.4	10.4	Ra-88	2	10.1	7.7
Al-13	3	28.5	17.8		2	18.8	14.6	Rb-37	1	4.18	4.18
As-33	3	28.4	18.9	Ho-67	3	22.8	13.6	Re-75	4	37.7	21.2
	5	62.6	33.9	I-53	5	(71)	(35)		7	(79)	(41)
At-85	5	(51)	(30)		7	(104)	(52)	Rh-45	3	31.1	18.9
	7	(91)	(46)	In-49	3	28	17.6		4	(46)	(26)
Au-79	1	9.23	9.23	Ir-77	3	(27)	(18)	Ru-44	3	28.5	17.5
	3	(30)	(20)		4	(39)	(23)		4	(46)	(25)
B-5	3	37.9	23.8	K-19	1	4.34	4.34		8	(119)	(58)
Ba-56	2	10	7.61	La-57	3	19.2	11.9	S-16	4	47.3	29
Be-4	2	18.2	13.8	Li-3	1	5.39	5.39		6	88	46.1
Bi-83	3	25.6	18.1	Lu-71	3	21	13.4	Sb-51	3	25.3	16.8
	5	56	33.1	Mg-12	2	15	11.3		5	56	30.1
Br-35	5	59.7	35.3	Mn-25	2	15.6	11.5	Sc-21	3	24.8	14.7
	7	103	52.6		3	33.7	18.9	Se-34	4	42.9	26.2
C-6	4	64.5	37		4	51.2	27		6	81.7	42.5
Ca-20	2	11.9	8.99		7	119	56.4	Si-14	4	45.1	25.8
Cd-48	2	16.9	13	Mo-42	3	27.2	16.8	Sm-62	3	23.4	13.4
Ce-58	3	20.2	12.2		4	46.4	24.2	Sn-50	2	14.6	11
	4	36.8	18.3		5	61.2	31.6		4	40.7	23.3
Cl-17	5	67.8	39.5		6	68	37.7	Sr-38	2	11	8.4
	7	114	58.4	N-7	3	47.4	30.5	Ta-73	5	(45)	(25)
Co-27	2	17.1	12.5		5	97.9	53.4	Tb-65	3	21.9	13.1
	3	33.5	19.5	Na-11	1	5.14	5.14	Tc-43	7	(94)	(46)
Cr-24	2	16.5	11.6	Nb-41	3	25	15.4	Te-52	4	37.4	23.2
	3	31	18.1		5	50.6	27		6	70.7	37.1
	6	90.5	43.9	Nd-60	3	22.1	12.8	Th-90	4	28.8	16.6
Cs-55	1	3.89	3.89	Ni-28	2	18.2	12.9	Ti-22	3	27.5	16
Cu-29	1	7.73	7.73		3	35.2	20.3		4	43.3	22.8
	2	20.3	14	O-8	6	138	72.2	Tl-81	1	6.11	6.11
Dy-66	3	22.8	13.5	Os-76	3	(25)	(17)		3	29.8	18.8
Er-68	3	22.7	13.6		4	(40)	(23)	Tm-69	3	23.7	14
Eu-63	2	11.2	8.45		8	(99)	(50)	U-92	6	(57)	
	3	24.9	13.9	P-15	3	30.2	20.1	V-23	2	14.7	10.7
F-9	7	185	94.1		5	65	35.4		3	29.3	16.9
Fe-26	2	16.2	12	Pb-82	2	15	11.2		4	46.7	24.4
	3	30.7	18.2		4	42.3	24.2		5	65.2	32.5
Fr-87	1	3.98	3.98	Pd-46	2	19.4	13.9	W-74	6	(61)	(32)
Ga-31	3	30.7	19.1		3	32.9	20.2	Y-39	3	20.5	13
Gd-64	3	20.6	12.9	Pm-61	3	22.3	12.9	Yb-70	3	25	14.5
Ge-32	2	15.9	11.9	Po-84	4	(38)	(23)	Zn-30	2	18	13.7
	4	45.7	25.9	Pr-59	3	21.6	12.5	Zr-40	4	34.3	19.3
H-1	1	13.6	13.6	Pt-78	2	18.6	13.8				

Source: Dean (1985); Samsonov (1973) in parentheses.
Note: Energies in units of eV/electron.

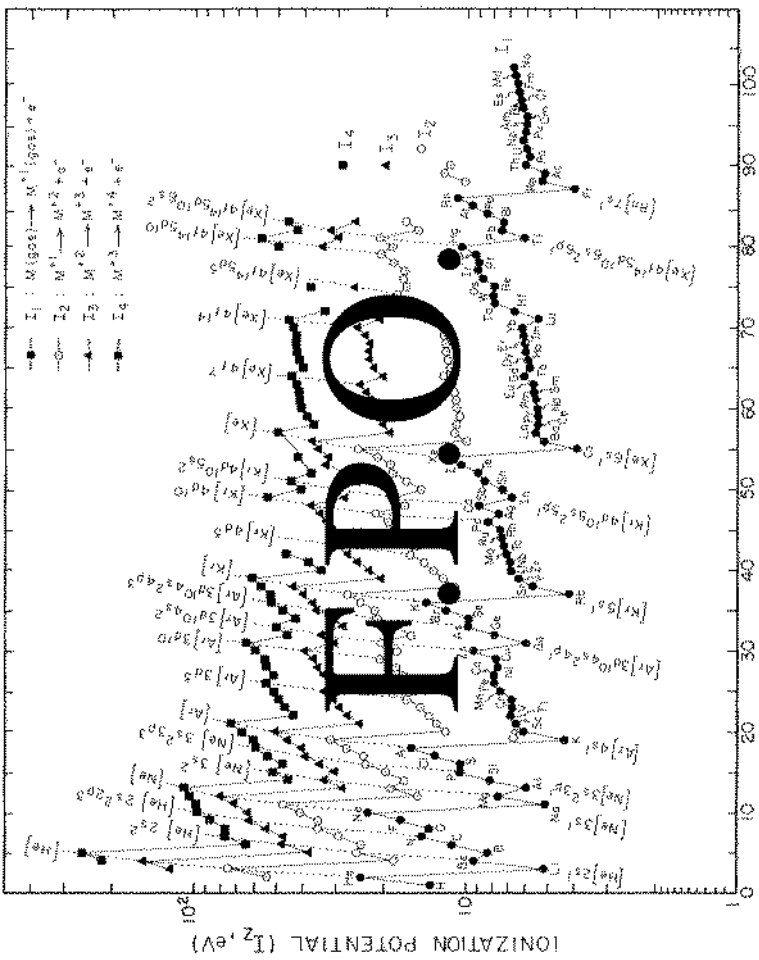

FIGURE I-9. First to fourth ionization energies (I_1 to I_4) as a function of Z. The maxima are always associated with full or half-full electron configurations.

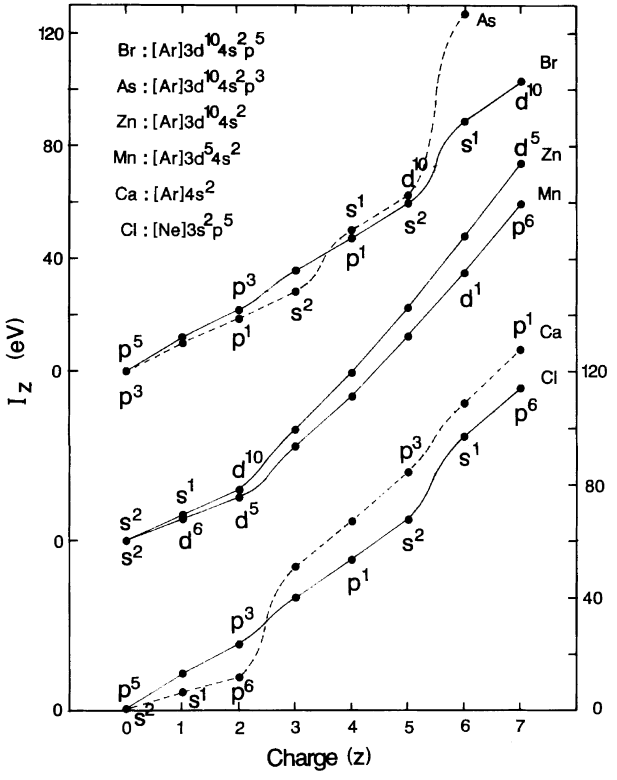

FIGURE I-10. Ionization energy (I_z) as a function of charge z for different gaseous elements. Notice that the slope changes at the full or half-full outermost subshells.

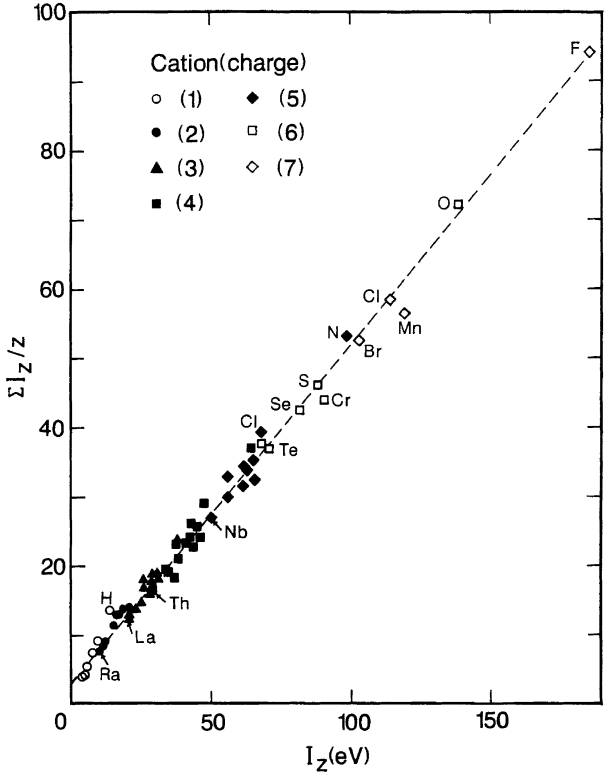

FIGURE I-11. The linear correlation between the average electron binding energy $\left(\sum I_z/z\right)$ and the electron binding energy I_z for various cations.

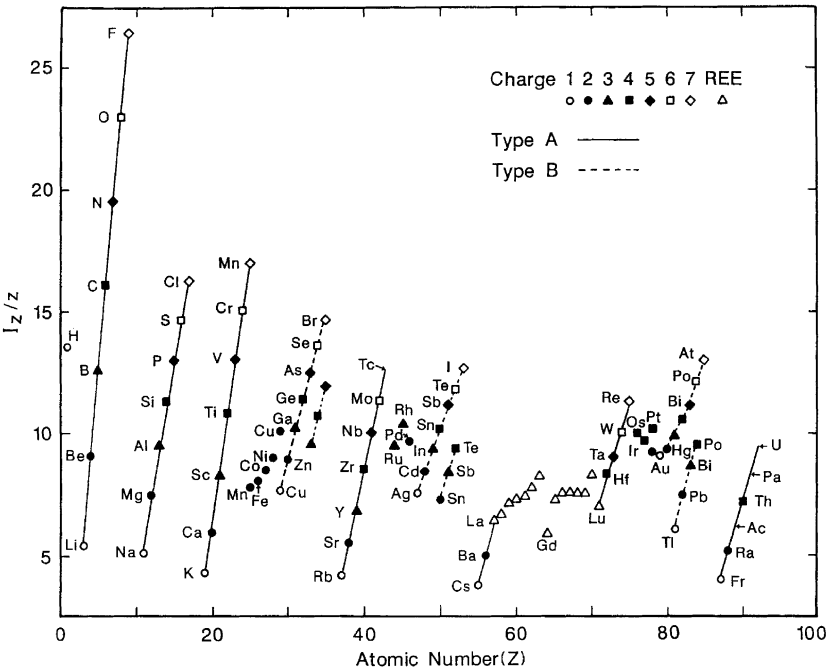

FIGURE I-12. Periodicity of polarizing power (I_z/z) as a function of atomic number Z.

I-5. IONIC RADII AND IONIC POTENTIALS

Ionic radii are derived from interatomic distances in oxides and fluorides (i.e., so-called ionic crystals), which consist of frameworks of cations and anions. One sets the ionic radius of O^{-2} with a coordination number of 6 (octahedral coordination) equal to 1.40 Å and assumes an additivity of ionic radii. Table I-4 summarizes the ionic radii (in Å) for sixfold coordination given by Shannon (1976), who revised and updated the earlier compilation by Shannon and Prewitt (1969) and adopted some values from Ahrens (1952). Though the ionic radii change with the coordination number (Shannon and Prewitt, 1969), it is still useful for comparison purposes to consider the ionic radii for the sixfold coordination as an intrinsic property of ions.

According to crystal field theory, when a transition metal cation is surrounded by six negatively charged ligands (e.g., O^{-2}) in octahedral coordination in a crystal, the energy level of the outermost *d* subshell is split in two with two orbitals at the higher energy level (e_g) and three orbitals at the lower energy level (t_{2g}). The energy separation between e_g and t_{2g} is called the **crystal field splitting parameter** Δ . The magnitude of Δ depends on the

TABLE I-4
Ionic radii (Å) for sixfold coordination

Z	z	r	Z	z	r	Z	z	r	Z	z	r
Ac-89	3	1.12		3L	0.54	Ni-28	2	0.69A		4	0.37A
Ag-47	1	1.15	Dy-66	2	1.07		3L	0.56		6	0.29A
	2	0.94		3	0.91A		3H	0.6	Sb-51	−3	2.45P
	3	0.75	Er-68	3	0.89A		4L	0.48		3	0.76A
A1-13	3	0.54	Eu-63	2	1.17	Np-93	2	1.1		5	0.6
Am-95	3	0.98		3	0.95		3	1.01	Sc-21	3	0.75
	4	0.85	F-9	−1	1.33A		4	0.87	Se-34	−2	1.98P
As-33	−3	2.22P		7	0.08A		5	0.75		4	0.50A
	3	0.58A	Fe-26	2L	0.61		6	0.72		6	0.42A
	5	0.46A		2H	0.78	O-8	−2	1.40A	Si-14	−4	2.71P
At-85	7	0.62A		3L	0.55		6	0.10A		4	0.4
Au-79	1	1.2a		3H	0.65A	OH	−1	1.37	Sm-62	3	0.96
	3	0.7a	Fr-87	1	1.80A	Os-76	4	0.63	Sn-50	−4	2.94P
	5	0.57	Ga-31	3	0.62A		5	0.58		2	0.93A
B-5	3	0.27	Gd-64	3	0.94		6	0.55		4	0.69
Ba-56	2	1.35A	Ge-32	−4	2.72P		7	0.53	Sr-38	2	1.18
Be-4	2	0.45		2	0.73A	P-15	−3	2.12P	Ta-73	3	0.72
Bi-83	3	1.03		4	0.53A		3	0.44A		4	0.68
	5	0.72a	Hf-72	4	0.71		5	0.34A		5	0.64
Bk-97	3	0.96	Hg-80	1	1.19	Pa-91	3	1.04	Tb-65	3	0.92A
	4	0.83		2	1.02		4	0.9		4	0.76
Br-35	−1	1.96P	Ho-67	3	0.90A		5	0.78	Tc-43	4	0.63a
	5	0.47A	1-53	−1	2.2	Pb-82	2	1.19A		5	0.6
	7	0.39A		5	0.62A		4	0.78		7	0.56A
C-6	−4	2.60P		7	0.53	Pd-46	2	0.86	Te-52	−2	2.21P
	4	0.16A	In-49	3	0.80A		3	0.71a		4	0.67a
Ca-20	2	1.00A	Ir-77	3	0.68A		4	0.62		6	0.56A
Cd-48	2	0.95		4	0.63	Pm-61	3	0.97	Th-90	4	0.94
Ce-58	3	1.01		5	0.57	Po-84	4	0.94	Ti-22	2	0.86
	4	0.87	K-19	1	1.38		6	0.67A		3	0.67
Cf-98	3	0.95	La-57	3	1.03	Pr-59	3	0.99		4	0.61
	4	0.82	Li-3	1	0.76		4	0.85	Tl-81	1	1.5
Cl-17	−1	1.81P	Lu-71	3	0.86A	Pt-78	2	0.80A		3	0.89
	5	0.34A	Mg-12	2	0.72		4	0.63	Tm-69	2	1.03
	7	0.27A	Mn-25	2L	0.67		5	0.57		3	0.88A
Cm-96	3	0.97		2H	0.83	Pu-94	3	1	U-92	3	1.03
	4	0.85		3L	0.58		4	0.86		4	0.89
Co-27	2L	0.65		3H	0.70a		5	0.74		5	0.76
	2H	0.75		4	0.53		6	0.71		6	0.73
	3L	0.55		7	0.46A	Ra-88	2	1.43A	V-23	2	0.79
	3H	0.61	Mo-42	3	0.69	Rb-37	1	1.52		3	0.64
	4L	0.49a		4	0.65	Re-75	4	0.63		4	0.58
	4H	0.53		5	0.61		5	0.58		5	0.54
Cr-24	2L	0.73		6	0.59		6	0.55	W-74	4	0.66
	2H	0.8	N-7	−3	1.71P		7	0.53		5	0.62
	3	0.62A		3	0.16A	Rh-45	3	0.67A		6	0.58a
	4	0.55		5	0.13A		4	0.6	Y-39	3	0.9
	5	0.51a	Na-11	1	1.02		5	0.55	Yb-70	2	1.02
	6	0.49a	Nb-41	3	0.72	Ru-44	3	0.68		3	0.87A
Cs-55	1	1.67A		4	0.68		4	0.62	Zn-30	2	0.74A
Cu-29	1	0.96A		5	0.64		5	0.57	Zr-40	4	0.72
	2	0.73A	Nd-60	3	0.98	S-16	−2	1.84P			

Notes: A: Ahrens' (1952) values adopted by Shannon (1976) or in agreement with Shannon's values within ±0.01; P: Pauling's Table 13-3 (1960); a: preferred interpolated values from Figure I-13. L: low spin; H: high spin. Some more ionic radii data are given by Dean (1985) though the data sources are not indicated.

nature of the ligands coordinated to the transition metal cation. The effect of crystal field splitting is to cause d subshell electrons to fill in first the lower energy level t_{2g} and then e_g, if Δ is large. On the other hand, the electric repulsion among electrons tends to cause electrons to be distributed first in all orbitals of d subshells with parallel spins, if the Δ is small. These two possibilities lead to **high**- and **low-spin electron configurations** for transition metal cations as shown in Table I-5. In oxides and silicates, those transition metal cations are in high-spin configuration. Burns (1970) discusses crystal field splitting under different coordination numbers of ligands and the application of crystal field theory to many geochemical problems.

As shown in Figure I-13, the radii of cations (for sixfold coordination; Shannon, 1976) with identical electron configuration decrease systematically with increasing charge of the cation. This can be explained by the contraction of the electron sheath by the increasing nuclear charges. The radii of A- and B-type cations with the same charge increase with the principal quantum number n, as one would have expected from the addition of new subshells. The radii of transition metal cations with identical charge and low-spin configurations decrease initially with increasing number of electrons in the outermost d subshell and then increase steadily when the d subshell electrons increase to more than 5 or 6. Also, the high-spin cations (open circles) are always larger than the low-spin cations (solid circles). In contrast, the radii of the lanthanide and actinide cations with identical charge decrease steadily when the number of electrons in the outermost f subshell increases. These phenomena are often called the **lanthanide** and **actinide contractions** (Goldschmidt, 1954). Apparently, the net effect of adding one electron to the electron sheath and one proton to the nucleus of lanthanides and actinides is a slight contraction of the electron sheath. The important consequence

TABLE I-5
Electron configurations of transition metal cations in octahedral coordination

No. of 3d electron	*Cation*			*High spin*		*Low spin*	
	$z = 2$	$z = 3$	$z = 4$	t_{2g}	e_g	t_{2g}	e_g
1		Ti	V	↑		↑	
2	Ti	V	Cr	↑ ↑		↑ ↑	
3	V	Cr	Mn	↑ ↑ ↑	↑	↑ ↑ ↑	
4	Cr	Mn		↑ ↑ ↑	↑ ↑	↑↓ ↑ ↑	
5	Mn	Fe		↑ ↑ ↑	↑ ↑	↑↓ ↑↓ ↑	
6	Fe	Co	Ni	↑↓ ↑ ↑	↑ ↑	↑↓ ↑↓ ↑↓	
7	Co	Ni		↑↓ ↑↓ ↑	↑ ↑	↑↓ ↑↓ ↑↓	↑
8	Ni			↑↓ ↑↓ ↑↓	↑ ↑	↑↓ ↑↓ ↑↓	↑ ↑
9	Cu			↑↓ ↑↓ ↑↓	↑↓ ↑	↑↓ ↑↓ ↑↓	↑↓ ↑
10	Zn	Ga	Ge	↑↓ ↑↓ ↑↓	↑↓ ↑↓	↑↓ ↑↓ ↑↓	↑↓ ↑↓

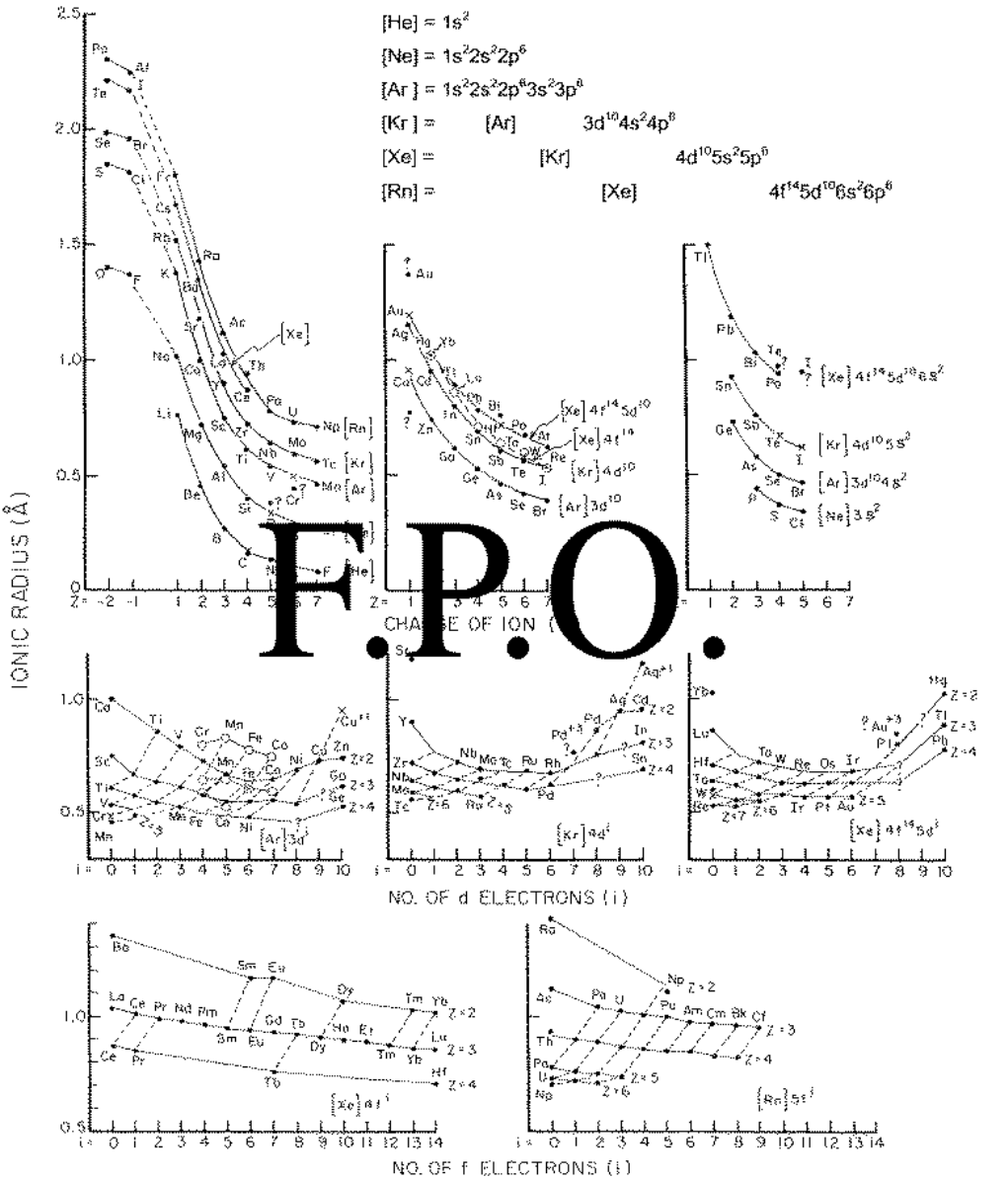

FIGURE I-13. Smooth systematic variations of ionic radii (r) as functions of electron configurations and charges. The question marks indicate doubtful data from Shannon (1976) and the crosses are the preferred values.

of the lanthanide contraction is that the ionic radii of the second and third series of transition metals become similar. Therefore, the Y-Lu, Zr-Hf, Nb-Ta, Mo-W, Ru-Os, Rh-Ir, Pd-Pt, and Ag-Au pairs often exhibit strikingly similar geochemical behavior.

Some data points given by Shannon (1976) do not fall on the smooth curves in Figure I-13 (indicated by question marks beside the data points), probably indicating unreliable data. The preferred ionic radii for those points are indicated by the crosses in the figure and by letter a in Table I-4.

The cationic charge z divided by its ionic radius r is called the **ionic potential** of the cation (Cartledge, 1928, 1930). Physically, the ionic potential, z/r, can be visualized as a quantity related to the energy required to separate an electron with charge of one from a positive point charge z at distance r to infinity, since this energy is equal to

$$\int_r^\infty ze^2/r^2\,dr = e^2\,z/r.$$

As discussed earlier, the zth ionization energy, I_z, is equivalent to the binding energy of an electron to a cation M^{+z}. Therefore, one would expect that z/r and I_z are somehow closely related, as shown in Figure I-14 (r is from Table I-4). For cations with identical electron configuration (connected by solid and dashed lines), I_z is equal to $a(z/r)^b$, where a is the intercept on the I_z axis at $z/r = 1$, and b is the slope of the straight lines in Figure I-14. One exception is the line connecting cations with [Ne] configuration (Li^+ to F^{+7}), where the slope exhibits a distinct break at Be^{+2}. Whether this break is real or not is uncertain. However, if one adopts the ionic radii of Be^{+2} (0.35 Å) and B^{+3} (0.23 Å) given by Ahrens (1952), the break disappears. Also, using only the r given by Ahrens (1952), the relationship $I_z = a(z/r)^b$ always holds. The slope, b, is not exactly equal to one, but not far from it (0.78 to 1.11). Comparing cations with the same charge (up to charge 4), I_z for B-type, transition and lanthanide metal cations is always higher than for A-type cations at similar z/r values. In short, the ionic potential alone cannot fully represent the interaction energy between cations and an electron. After all, a cation M^{+z} is not a simple sphere with a radius of r and a point charge of z at the center.

For comparison, Figure I-15 summarizes the ionic radii as a function of ionic charge and the types of electron configurations (A-, B-types, etc.). In hard rock geochemistry, we mostly deal with silicates and oxides. Therefore the high-spin radii of divalent and trivalent Mn, Fe, Co, and Ni are adopted in Figure I-15. Ions with similar ionic radius and charge can often substitute for one another in a mineral structure, thus exhibiting similar geochemical behavior. For example, in olivine ($[Mg, Fe]_2SiO_4$), the Mg and Fe can easily be substituted by Ni, Co, Mn, and Zn, since they have very similar ionic radii and identical charge. In chromite ($FeCr_2O_4$), the noble metals are enriched

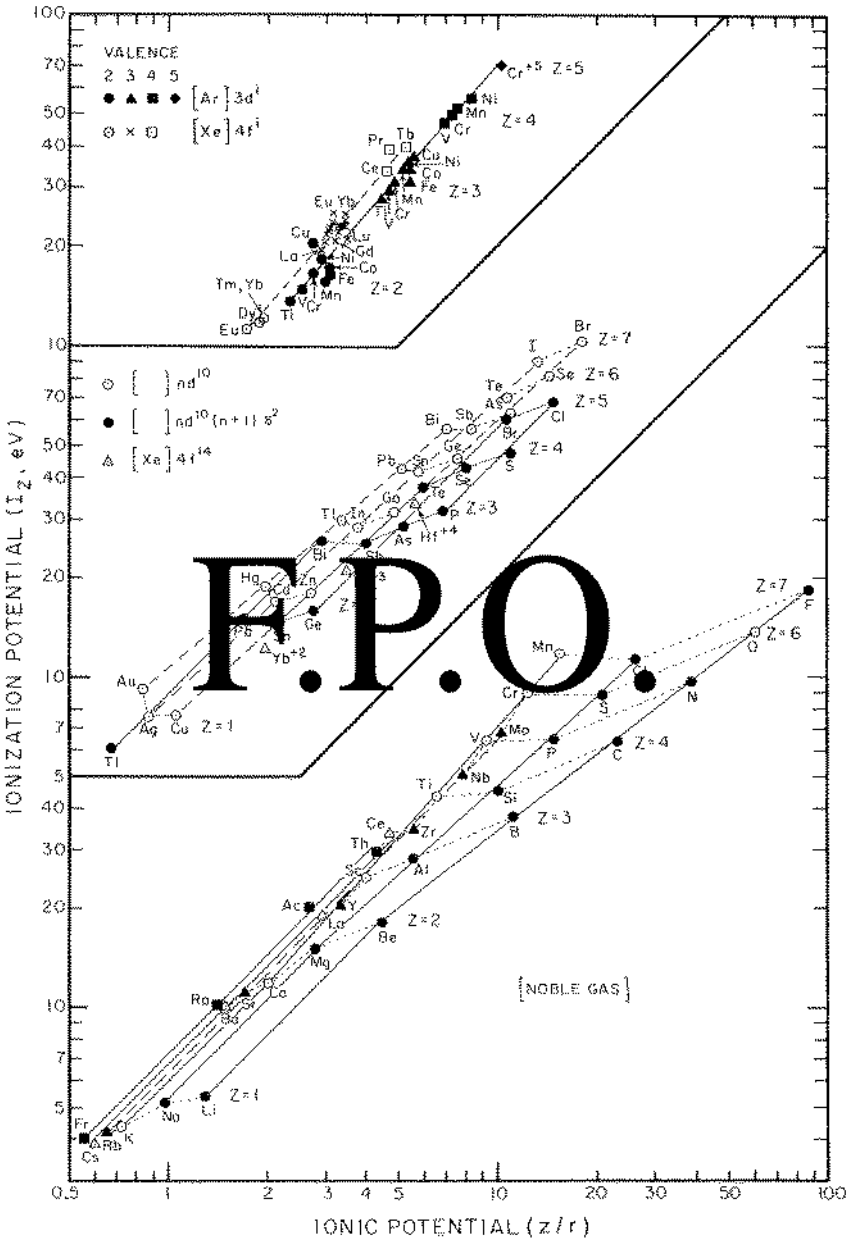

FIGURE I-14. Plots of ionic potentials (z/r) versus the electron binding energies (I_z) for cations with different electron configurations. Data are from Tables I-3 and I-4.

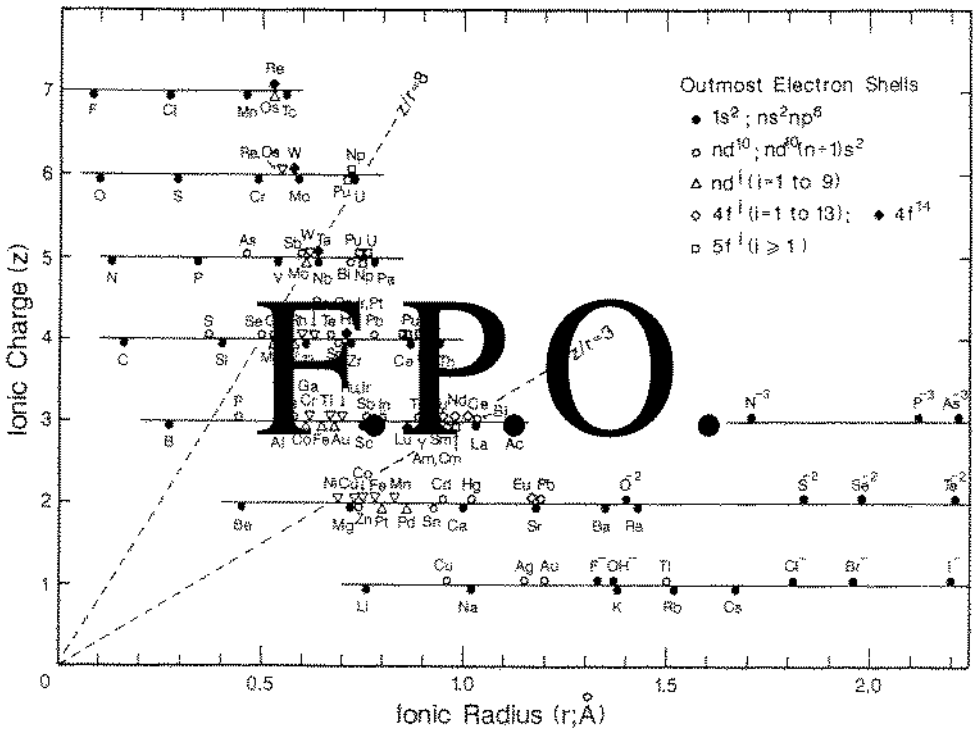

FIGURE I-15. Ionic radii (r) as functions of charges and electron configurations of outermost subshells.

because the ionic radii of Cr^{+3} and tri- and tetravalent noble metal cations are similar. Similarly, ilmenite ($FeTiO_3$) is often enriched in V, Hf-Zr, and Nb-Ta pairs. Also Y-REE (rare earth elements) and W-Mo pairs are closely associated in nature. Nonetheless, one should not predict the geochemical behavior of elements by ionic radius and charge alone. For example, according to ionic radius and charge, the B-type Cu^{+}, Ag^{+}, Au^{+}, Sn^{+2}, Cd^{+2}, and Hg^{+2} cations can easily substitute for K^{+}, Na^{+}, and Ca^{+2} in alkali and plagioclase feldspars of igneous rock. However, the concentrations of those B-type cations in these minerals are usually very low, because they may already have been segregated from the magma as sulfide minerals.

In general, cations with an ionic potential (z/r) of less than 3 exist as dissolved cations, with $8 > z/r > 3$ as least soluble hydroxide precipitates, and with $z/r > 8$ as dissolved oxyanions in oxygenated aqueous solutions (Mason, 1966a).

I-6. Electric Polarizability

Under the influence of an external electric field, E, the electron sheath around an atom is deformed to form an electric dipole moment, μ, which is proportional to E. The proportionality constant, k_α, is called the **electric polarizability**, i.e., $\mu = k_\alpha \cdot E$. The electric polarizability has units of volume (10^{-24} cm^3/atom or ion). The k_α values for some A- and B-type ions are summarized in Table I-6 (Pauling, 1927). For ions with the same electron configuration, k_α decreases systematically from the highly charged anions to the highly charged cations (Table I-6). Comparing cations with the same charge, the k_α for B-type cations (and probably transition metal cations) is always much higher than for A-type cations with similar ionic radii, as exemplified in Figure I-16. In other words, the electron sheaths of A-type cations are spherically symmetric and hard to deform under the electric field (low polarizability), whereas the electron sheaths of B-type and transition metal cations are highly polarizable, especially in the d subshell electrons. Since the electric polarizability of the S^{-2} anion is much higher than that of the O^{-2} anion (10.3 vs. 3.92×10^{-24} cm^3/ion in Table I-6), the B-type and some transition metal cations tend to form sulfides with strong covalent characteristics (i.e., electron pair sharing). A-type cations form oxides with strong ionic bond characteristics (i.e., electrostatic attraction between cation and anion). Also, the complexation constants of a given B-type cation with various ligands are in the order of $P^{-3} > N^{-3}$; $S^{-2} > O^{-2}$; $I^- > Br^- > Cl^- > F^-$ (in increasing order of k_α), and $NO_3^- > CO_3^{-2}$; $ClO_4^- > SO_4^{-2} > PO_4^{-3}$ (in decreasing order of k_α). The order is reversed for A-type cations (Stumm and Morgan, 1981).

One may consider a reaction

$$\frac{1}{z}M_2O_z(s) + S(s) \leftrightarrow \frac{1}{z}M_2S_z(s) + \frac{1}{2}O_2(g).$$

Its equilibrium constant is $K = P_{O_2}^{1/2} = \exp(-\Delta\tilde{G}/RT)$, or

$$-RT \ln K = -\frac{RT}{2} \ln P_{O_2} = \Delta\tilde{G} = (\Delta G_f^0 M_2S_z - \Delta G_f^0 M_2O_z)/z,$$

where $\Delta\tilde{G}$ is the Gibbs free energy of the reaction, $\Delta G_f^0 M_2S_z$ and $\Delta G_f^0 M_2O_z$ are the Gibbs free energies of formation for M_2S_z and M_2O_z solids, and z is the valence of M; for $z = 2$ and 4, $\Delta G_f^0 M_2O_z$ (or $\Delta G_f^0 M_2S_z$) is equivalent to 2 $\Delta G_f^0 MO$ and 2 $\Delta G_f^0 MO_2$, respectively. The calculated ($\Delta G_f^0 M_2S_z - \Delta G_f^0 M_2O_z)/z$ values for B-type and transition metal cations are summarized in Table I-7 (see page 38). The term $(\Delta G_f^0 M_2S_z - \Delta G_f^0 M_2O_z)/z$ is a measure of the relative affinity of cations for sulfides over oxides, or a measure of the **relative polarizability** of cations. The more negative the ($\Delta G_f^0 M_2S_z -$

TABLE I-6
Electric polarizability K_α

z												*Electron configuration*
−4	−3	−2	−1	0	1	2	3	4	5	6	7	
			H	He	Li	Be	B	C	N			[He]
			10.17	0.203	0.029	0.0079	0.003	0.0013	0.0007			
C	N	O	F	Ne	Na	Mg	Al	Si	P	S	Cl	[Ne]
2140	28.8	3.92	1.05	0.394	0.181	0.094	0.054	0.033	0.021	0.014	0.01	
Si	P	S	Cl	Ar	K	Ca	Sc	Ti	V	Cr	Mn	[Ar]
377	41.6	10.3	3.69	1.64	0.84	0.472	0.29	0.19	0.12	0.087	0.063	
					Cu	Zn	Ga	Ge	As	Se	Br	[Ar]$3d^{10}$
					0.43	0.29	0.2	0.14	0.1	0.075	0.059	
Ge	As	Se	Br	Kr	Rb	Sr	Y	Zr	Nb	Mo		[Kr]
109	28.8	10.6	4.81	2.48	1.42	0.86	0.56	0.38	0.26	0.19		
					Ag	Cd	In	Sn	Sb	Te	I	[Kr]$4d^{10}$
					1.72	1.09	0.73	0.5	0.36	0.26	0.19	
Sn	Sb	Te	I	Xe	Cs	Ba	La	Ce				[Xe]
90.4	31.9	14.1	7.16	4.03	2.44	1.56	1.05	0.74				
					Au	Hg	Ti	Pb	Bi			[Xe]$4f^{14}\,5d^{10}$
					1.88	1.24	0.87	0.62	0.46			

Note: Units are 10^{-24} cm^3/atom or ion.

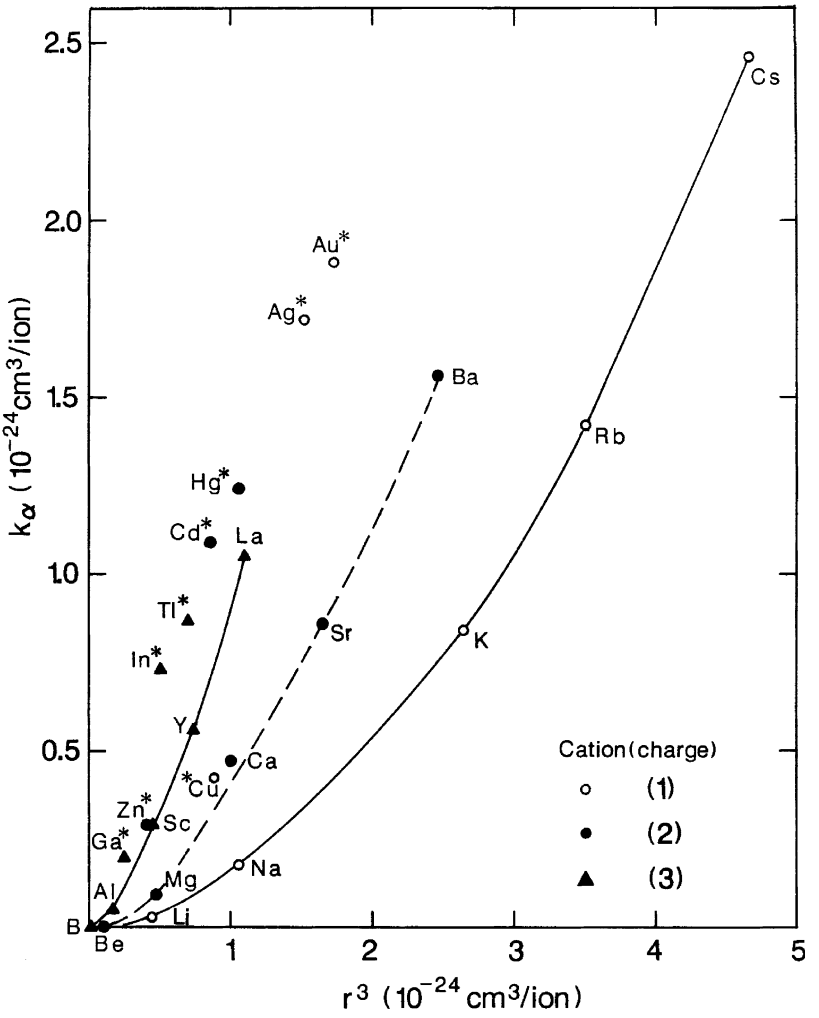

FIGURE I-16. Electric polarizability of cations (k_α) as a function of the cube of the ionic radius and the charge. Notice that the B-type cations (with asterisk) always fall above the lines connecting the A-type isovalent cations.

$\Delta G^0_f M_2O_z)/z$ values, the higher the equilibrium partial pressure of oxygen, (P_{O_2}), the higher the affinity to sulfides, and the higher the relative polarizability of cations. The relative polarizabilities of Cu^+, Cu^{+2}, Ag^+, Au^+, Au^{+3}, Hg^+, Hg^{+2}, Pd^{+2}, Pt^{+2}, Pt^{+4}, Tl^{+3}, Ir^{+3}, Ir^{+4}, Rh^{+3}, Os^{+4}, and Ru^{+4} are high as shown in Table I-7. These cations also form strong complexes with organic ligands and are highly toxic to living organisms, in part due to their blockage of vital functional groups in biomolecules (Ochiai, 1987).

TABLE I-7
$(\Delta G_f^0 M_2S_z - \Delta G_f^0 M_2O_z)/z$ values for B-type and transition metal cations

	$n = 3$				$n = 4$				$n = 5$			
	$z = 1$	2	3	4	$z = 1$	2	3	4	$z = 1$	2	3	4
nd^1		Sc	Ti									
			55									
nd^2		Ti	V					Mo				W
		53	51					37				41
nd^3		V	Cr					Tc				Re
		48	58					20				24
nd^4								Ru				Os
								8				8
nd^5		Mn	Fe									Ir
		37	39									−1
nd^6		Fe					Rh				Ir	Pt
		34					−4				−3	−3
nd^7		Co										
		31										
nd^8		Ni				Pd				Pt		
		32				−1				−8		
nd^9		Cu										
		17										
nd^{10}	Cu	Zn	Ga	Ge	Ag	Cd	In	Sn	Au	Hg		
	11	28	38	43	−7	18	33	42		2		
$nd^{10}\,s^1$									Hg			
									7			
$nd^{10}\,s^2$		Ge	As			Sn	Sb		Tl	Pb	Bi	
		33	35			31	34		13	22	28	

Source: Thermodynamic data are mainly from Dean (1985), Karapet'yants and Karapet'yants (1970), Mills (1974), and Wagman et al. (1982).

Note: Units are kcal/mole.

I-7. ELECTRONEGATIVITY

Pauling (1932, 1960) described qualitatively the **electronegativity**, χ, as "the power of an atom in a molecule to attract electrons to itself." Therefore, we would again expect a close relationship between the electronegativity and the electron binding energy. According to Pauling (1932, 1960), the electronegativity difference between two unlike atoms of nonmetals A_i and A_j is related by the following equation:

$$\alpha \cdot (\chi_{A_i} - \chi_{A_j})^2 = D(A_i \leftrightarrow A_j) - \{D(A_i \leftrightarrow A_i) + D(A_j \leftrightarrow A_j)\}/2, \quad \text{(I-3a)}$$

where $D(A_i \leftrightarrow A_j)$ is the single bond energy between two unlike atoms in a gaseous molecule, $D(A_i \leftrightarrow A_i)$ or $D(A_j \leftrightarrow A_j)$ is the single covalent bond energy between two identical atoms in a diatomic or polyatomic gaseous molecule, and α is a proportionality constant with the dimension of energy. Therefore, according to equation I-3a, the electronegativities of atoms are dimensionless.

The $D(A_i \leftrightarrow A_j)$ values, including $i = j$, for many gaseous compounds containing nonmetals and hydrogen at the standard state can be obtained by thermochemical and spectroscopic methods and are listed by Pauling (1960) and Pauling and Pauling (1975). By assigning 2.5 and 4.0 as the electronegativities of carbon and fluorine, respectively, Pauling obtained an α value of 23 kcal/mole and the χ_A values for other nonmetals and hydrogen, as summarized in Table I-8. Even though he mentioned that his electronegativity values for the elements refer to the most common oxidation states of the elements, he did not explicitly assign the oxidation states. One can, however, infer the oxidation states of elements for each χ_A from the gaseous compound by which the $D(A_i \leftrightarrow A_j)$ value is estimated, assuming the fluorine atom in the gaseous compound is always a monovalent anion. The inferred oxidation states of the nonmetals are also given in Table I-8. As discussed by Pauling (1960), the larger the electronegativity difference between two unlike nonmetal atoms, the stronger the ionic bond or the weaker the covalent bond characteristics (independent of the bond strength itself).

The metals usually cannot exist as diatomic gases (except for alkali metals), and metal-nonmetal compounds are mostly solid or liquid at the standard state. Therefore, one cannot apply equation I-3a to obtain the electronegativity of metal atoms (χ_M). Pauling (1960) postulated, however, that

$$\alpha \cdot (\chi_M - \chi_A)^2 = \frac{-(\Delta H_f M_m A_n)}{m \cdot n}, \quad \text{(I-3b)}$$

TABLE I-8
The electronegativities of metal cations $(\chi_{M^{+z}})$ and nonmetal ions (χ_{A^z})

Z	z	$\chi_{M^{+z}}$	Z	z	$\chi_{M^{+z}}$	Z	z	$\chi_{M^{+z}}$	Z	z	$\chi_{M^{+z}}$
Ac-89	3	1	Ga-31	3	1.6	Pd-46	2	2	Tl-81	1	1.5
Ag-47	1	1.8	Gd-64	3	*1.1		3	*2.1		3	1.9
Al-13	3	1.5	Ge-32	4	1.8	Pm-61	3	*1.1	Tm-69	3	*1.1
Am-95	3	*1.1	Hf-72	4	1.4	Po-84	4	2	U-92	4	1.4
As-33	3	2	Hg-80	1	*1.7	Pr-59	3	*1.1		6	*1.6
	5	2.1		2	1.8	Pt-78	1–4	*2.2	V-23	3	*1.55
At-85	5	2.2	Ho-67	3	*1.1	Pu-94	3,4	1.1		4	1.7
Au-79	3	2.3	In-49	1	*1.5	Ra-88	2	*0.85		5	1.9
B-5	3	2		3	*1.6	Rb-37	1	0.8	W-74	2	*1.8
Ba-56	2	0.9	Ir-77	3,4	2.2	Re-75	3	*2.0		4	*1.9
Be-4	2	1.5	K-19	1	0.8		5	*2.1		6	2.0
Bi-83	3	1.8	La-57	3	1.1		7	2.2	Y-39	3	1.2
C-6	4	2.5	Li-3	1	0.95	Rh-45	2,3	2.1	Yb-70	2	*1.0
Ca-20	2	1	Lu-71	3	1.15	Ru-44	3	*2.1		3	*1.2
Cd-48	2	1.5	Mg-12	2	1.2	S-16	2,4	*2.5	Zn-30	2	1.5
Ce-58	3	1.1	Mn-25	2	1.5		6	(2.3)	Zr-40	4	1.4
	4	*1.4		3	*1.7	Sb-51	3	1.9			
Cl-17	7	(2.5)		7	2.5		5	2.1			
Cm96	3	*1.2	Mo-42	2	*1.8	Sc-21	3	1.3			
Co-27	2	1.8		4	*1.9	Se-34	4	*2.4	*Nonmetal ions*		
	3	1.9		6	*2.0	Si-14	4	1.8	Z	z	χ_{A^z}
Cr-24	2	1.5	N-7	5	(3)	Sm-62	2	*1.0			
	3	1.6	Na-11	1	0.9		3	*1.1	As-33	3	2
	6	2.2	Nb-41	3	*1.5	Sn-50	2	1.7	Br-35	−1	2.8
Cs-55	1	0.75		5	*1.7		4	1.8	C-6	4	2.5
Cu-29	1	1.8	Nd-60	3	1.1	Sr-38	2	1	Cl-17	−1	3
	2	2	Ni-28	2	1.8	Ta-73	3	*1.6	F-9	−1	4
Dy-66	3	*1.1		3	*1.9		5	1.7	H-1	1	2.1
Er-68	3	*1.1	O-8	6	(3.5)	Tb-65	3	*1.1	I-53	−1	2.5
Eu-63	2	*0.9	Os-76	3,4	2.2	Tc-43	7	2.3	N-7	3	3
	3	*1.2	P-15	3,5	2.1	Te-52	4	*2.1	O-8	−2	3.5
F-9	7	(4)	Pa-91	4	*1.35	Th-90	2	*1.1	P-15	3	2.1
Fe-26	2	1.7		5	*1.45		4	*1.2	S-16	−2	2.5
	3	1.8	Pb-82	2	1.6	Ti-22	2	1.4	Se-34	4	2.4
Fr-87	1	0.7		4	*2.0		4	1.6	Si-14	4	1.8

Source: Data are mainly from Gordy and Thomas (1956) and Pauling (1960) except for those with an asterisk, which are newly calculated. The $\chi_{M^{+z}}$ values in parentheses are extrapolated from Figure I-17.

Note: Z and z are the atomic number and the charge of the ions, respectively.

if A is a nonmetal other than oxygen and nitrogen, or

$$\alpha \cdot (\chi_M - \chi_A)^2 = \frac{-(\Delta H_f M_m A_n + a \cdot n)}{m \cdot n}, \qquad \text{(I-3c)}$$

if A is oxygen or nitrogen, where $\Delta H_f M_m A_n$ is the enthalpy of formation for a metal-nonmetal solid compound $M_m A_n$ at the standard state; n and m are the absolute values of the charge of metal M and nonmetal A, respectively, in the solid compound $M_m A_n$; α is 23 kcal/mole; and a is 26.0 kcal/mole for oxygen and 55.4 kcal/mole for nitrogen.

Because χ_A and α are already known, χ_M can be calculated from equations I-3b and I-3c if ΔH_f for a solid metal-nonmetal compound is known. The χ_M values given by Pauling (1960) and Gordy and Thomas (1956) are summarized in Table I-8 with some revisions and additions, using more recent ΔH_f data for chloride, bromide, and iodide compounds (Wagman et al., 1982; Dean, 1985; Karapet'yants and Karapet'yants, 1970). As exemplified in Table I-9, the χ_M values calculated from fluoride and oxide data for mono- to trivalent cations are very often much larger than those from other compound data. Therefore, strictly speaking, the χ_M values in Table I-8 are applicable only to chloride, bromide, iodide, sulfide, and selenide compounds, and not to every kind of solid compound. The corresponding oxidation states of metals for χ_M, as inferred from the solid compound $M_m A_n$, are also indicated in Table I-8. As suggested by Haissinsky (1946) and Gordy and Thomas (1956), the electronegativity for multivalent metals varies with valence (see Table I-8). Therefore, it will be more convenient to talk about the electronegativity of a cation, $\chi_{M^{+z}}$, than that of a neutral element hereafter. The fact that $\chi_{M^{+z}}$ are equal to $\chi_{A^{+z}}$ for metalloid elements (As, C, P, Se, and Si)

TABLE I-9
Electronegativities of cations calculated by equations I-3b and I-3c for halides, oxides, sulfieds, and selenides

	F^-	Cl^-	Br^-	I^-	O^{-2}	S^{-2}	Se^{-2}
Na^+	1.55	0.93	0.86	0.77	1.85	1.12	1.07
Mg^{+2}	1.58	1.17	1.15	1.12	1.58	1.16	1.21
Al^{+3}	1.71	1.44	1.47	1.46	1.64	1.38	1.41
Si^{+4}		1.66	1.7	1.8	1.79	1.76	
P^{+5}		2.04	2.05				
Cu^+	2.59	1.81	1.75	1.66	2.3	1.86	1.84
Zn^{+2}	1.99	1.53	1.49	1.46	1.54	1.5	1.48
Ga^{+3}	1.99	1.65	1.64	1.59	1.93	1.5	1.53
Ge^{+4}		1.82	1.85	1.89	1.8	1.86	
As^{+5}					2.26	2.11	

in Table I-8 proves the validity of equation I-3b as postulated by Pauling (1960).

As would be expected, the **cationic electronegativities** are linearly correlated with I_z/z values for the A-type cations, while B-type cations and transition metal cations with a more than half-full d subshell tend to have higher $\chi_{M^{+z}}$ values than those for A-type cations at a given I_z/z, value as shown in Figure I-17. Furthermore, the extrapolated $\chi_{M^{+z}}$ values for the A-type cations such as F^{+6}, O^{+6}, and N^{+5} in Figure I-17 are identical to χ_A values for F^-, O^{-2}, and N^{-3}. Therefore, the electronegativities for these elements are independent of charge. The periodicity of cationic electronegativities as a function

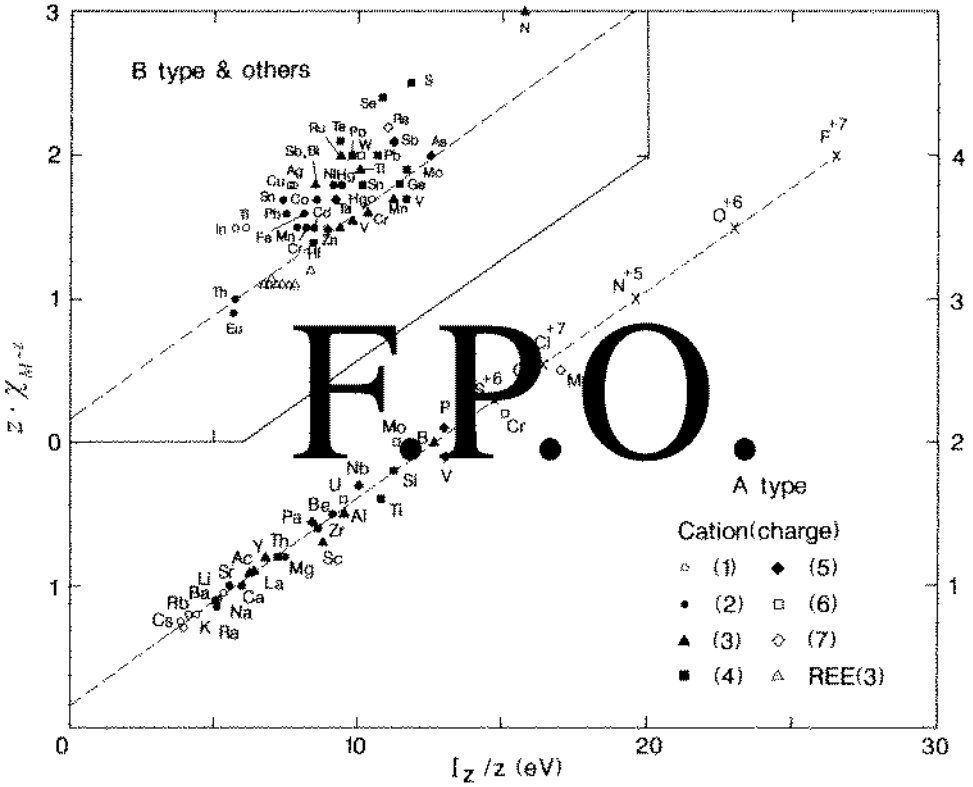

FIGURE I-17. Electronegativities of cations $(\chi_{M^{+z}})$ versus their polarizing powers (I_z/z). The crosses are extrapolated values. Data are from Tables I-3 and I-8.

of atomic number is shown in Figure I-18 and is very similar to the periodicity of I_z/z (Figure I-12).

Mulliken (1934) also defined the electronegativity of neutral elements as

$$\chi_M = \frac{I_1 + I_{-1}}{2}.$$

The original electronegativity scale by Pauling (his Table 3-8, 1960) is often assumed to be for the neutral elements and is compared with that by Mulliken (1934) as shown in Figure I-19. Though the general correlation between them is good, the scatter of O, H, B, Al, Ga, In, Tl, Pb, Bi, Cs, and many other transition metals is large, and those elements do not possess any common physicochemical property that explains the scatter.

In conclusion, Pauling's cationic electronegativity multiplied by cationic charge ($z \cdot \chi_{M^{+z}}$) is a quantity closely related to I_z for A-type cations. For

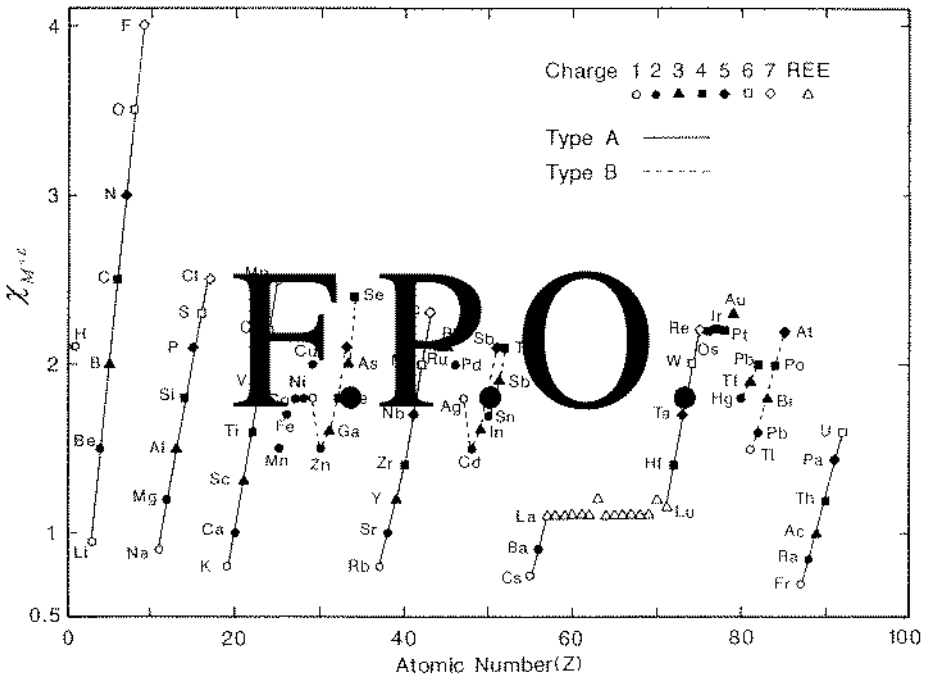

FIGURE I-18. Periodicity of the electronegativities of cations. Data are from Table I-8.

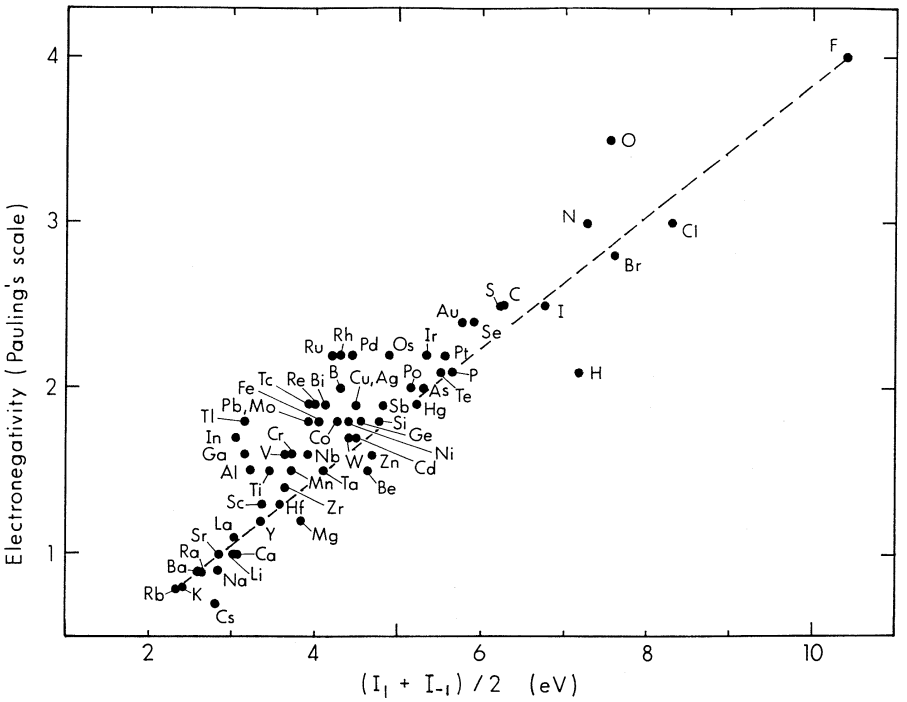

FIGURE I-19. Pauling's electronegativity scale versus Mulliken's $(I_1 + I_{-1})/2$.

B-type cations and some transitional metal cations, the I_z may underestimate the electron attraction power as compared to the corresponding $z \cdot \chi_{M^{+z}}$. We may call $z \cdot \chi_{M^{+z}}$ the **total cationic electronegativity**. As mentioned earlier, Pauling's electronegativity scale cannot apply to fluorides and oxides nor to silicates (Saxena, 1977). For those types of compounds, one has to adopt a new electronegativity scale specific to each type of compound, as Saxena (1977) did for silicates.

I-8. CRYSTAL LATTICE ENERGIES

The crystal lattice energy of a mineral, ΔH_L^0, is defined as the energy required to break up one mole of molecules in a crystalline form into gaseous cations and anions at 25°C and one bar. The anions can be monoatomic (e.g., O^{-2}, S^{-2}) or complex ions such as oxyanions (CO_3^{-2}, SiO_4^{-4}).

The ΔH_L^0 of an oxide M_mO_n can be estimated by using the Born-Haber cycle (Born and Lande, 1918; Born, 1919; Haber, 1919), i.e.,

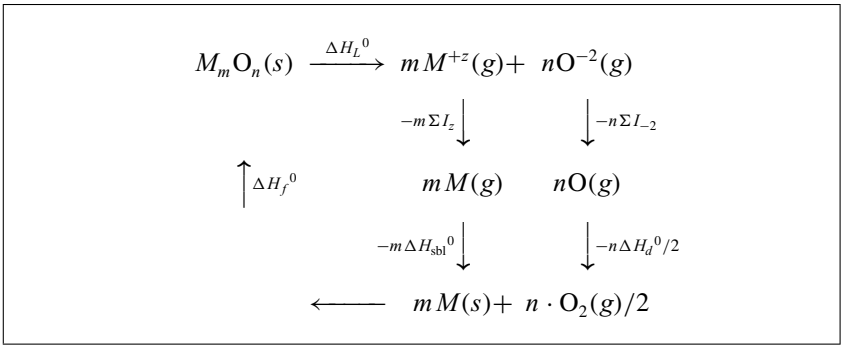

where m and n are the number of cations and oxygen atoms in the oxide formula, respectively. If the charge of the cation is z, then $m = 2n/z$; ΣI_z is the cumulative ionization energy of the metal M(g); ΔH_{sbl}^0 is the enthalpy of sublimation of the metal M(s); ΣI_{-2} is the affinity of two electrons to the gaseous oxygen atom = 601 kJ/mol; ΔH_d^0 is the enthalpy of dissociation of O_2 gas = 498 kJ/mol (Wagman et al., l982); and ΔH_f^0 is the enthalpy of formation of the oxide M_mO_n.

Since the total enthalpy change for the cycle is equal to zero, i.e.,

$$\Delta H_L^0 - m\left(\Sigma I_z + \Delta H_{\text{sbl}}^0\right) - n\left(\Sigma I_{-2} + \Delta H_d^0/2\right) + \Delta H_f^0 = 0,$$

then

$$\Delta H_L^0 = m\left(\Sigma I_z + \Delta H_{\text{sbl}}^0\right) + n\left(\Sigma I_{-2} + \Delta H_d^0/2\right) - \Delta H_f^0, \qquad \text{(I-4a)}$$

or

$$\Delta H_L^0/n = 2/z \cdot \left(\Sigma I_z + \Delta H_{\text{sbl}}^0\right) + \left(\Sigma I_{-2} + \Delta H_d^0/2\right) - \Delta H_f^0/n. \qquad \text{(I-4b)}$$

$\Delta H_L^0/n$ can be considered as a measure of relative chemical bond strength between oxygen and various metals (O-M).

In equation I-4b, the $(\Sigma I_{-2} + \Delta H_d^0/2)$ term for oxygen is constant (= 850 kJ/mol), and the $2\Sigma I_z/z$ term is always much larger than the $2\Delta H_{\text{sbl}}^0/z$ and $-\Delta H_f^0/n$ terms. Therefore, a near-linear correlation for oxides between $\Delta H_L^0/n$ (summarized in Table I-10) and $\Sigma I_z/z$ is expected, and is proven in Figure I-20. As shown before, $\Sigma I_z/z$ and I_z are linearly related (Figure I-11), therefore $\Delta H_L^0/n$ should also correlate nicely with I_z. In short, the O-M bond strength as represented by the crystal lattice energy, $\Delta H_L^0/n$, is closely related to the electron binding energy, I_z, which is in turn closely related to the total cationic electronegativity $z \cdot \chi_{M^{+z}}$.

TABLE I-10
Crystal lattice energies of oxides (M_mO_n) per one oxygen, $\Delta H_L^0/n$, as calculated by the Born-Haber cycle

Oxide	$\Delta H_L^0/n$	*Oxide*	$\Delta H_L^0/n$	*Oxide*	$\Delta H_L^0/n$	*Oxide*	$\Delta H_L^0/n$
Ag_2O	2930	Eu_2O_3	4220	MoO_2	6160	SnO	3570
Al_2O_3	5060	FeO	3860	MoO_3	8600	SnO_2	5800
As_2O_3	4830	Fe_2O_3	4920	Na_2O	2490	SrO	3230
B_2O_3	6260	Fr_2O	2120	NbO	4040	Tb_2O_3	4270
BaO	3060	Ga_2O_3	5090	NbO_2	5700	ThO_2	4980
BeO	4450	GeO	3750	Nd_2O_3	4150	TiO	3840
Bi_2O_3	4690	GeO_2	6330	NiO	4020	Ti_2O_3	4760
CaO	3410	HfO_2	5510	Ni_2O_3	5240	TiO_2	5970
CdO	3730	HgO	3830	P_2O_3	5075	Tl_2O	2580
Ce_2O_3	4090	Ho_2O_3	4310	P_2O_5	8010	Tl_2O_3	4710
CeO_2	5160	In_2O_3	4720	PbO	3440	Tm_2O_3	4340
CoO	3930	K_2O	2240	PbO_2	5760	VO	3870
Cr_2O_3	5000	La_2O_3	4050	PdO	4000	V_2O_3	4870
Cs_2O	2120	Li_2O	2820	Rb_2O	2180	VO_2	6180
Cu_2O	3210	Lu_2O_3	4370	ReO_2	5550	V_2O_5	7660
CuO	4070	MgO	3800	Rh_2O_3	4970	Y_2O_3	4300
Dy_2O_3	4280	MnO	3760	Sc_2O_3	4590	ZnO	3980
Er_2O_3	4330	Mn_2O_3	5020	SiO_2	6520	ZrO_2	5450
EuO	3260	MnO_2	6470	Sm_2O_3	4190		

Source: Thermodynamic data sources are the same as in Table I-7.
Note: All are in units of kJ/mol oxygen.

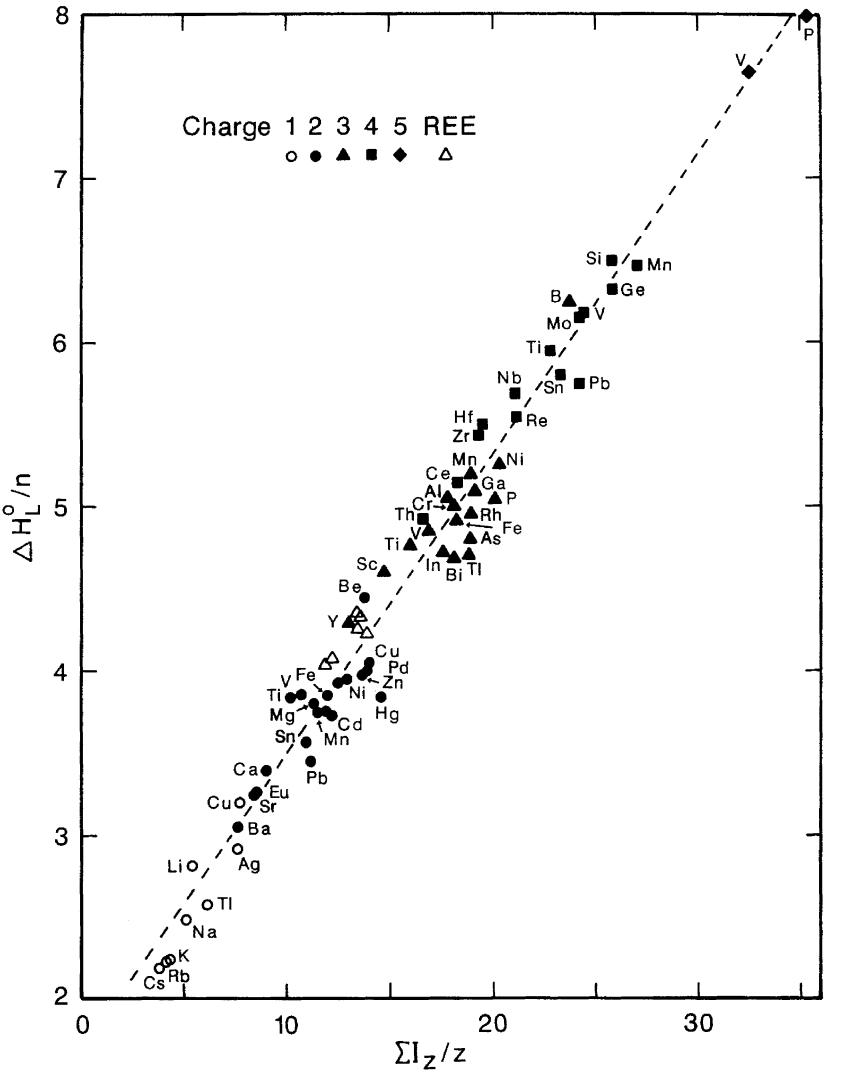

FIGURE I-20. Plot of crystal lattice energy for metal oxides divided by the number of oxygen atoms in the molar crystal formula $\left(\Delta H_L^0/n\right)$ versus the average electron binding energy $\left(\sum I_z/z\right)$ to metal cations.

I-9. Hydrolysis of Cations and Dissociation of Oxyacids

The hydrolysis of a cation M^{+z} in water can be represented by

$$M^{+z} + H_2O \rightarrow M(OH)^{z-1} + H^+,$$

$$M^{+z} + iH_2O \rightarrow M(OH)_i^{z-i} + iH^+,$$

where the first **hydrolysis constant** ${}^*K_1$ is defined by

$${}^*K_1 = \frac{[M(OH)^{z-1}] \cdot [H^+]}{[M^{+z}]}, \tag{I-5a}$$

and the ith cumulative hydrolysis constant ${}^*k_i$ by

$${}^*k_i = \frac{[M(OH)_i^{z-i}] \cdot [H^+]^i}{[M^{+z}]}. \tag{I-5b}$$

The ${}^*K_1$ values are summarized in Table I-11. The $\log {}^*K_1$ can be considered as a measure of relative bond strength between hydroxyl and metal ions (M-OH). The larger the $\log {}^*K_1$ value, the higher the tendency for the cation to form a hydroxide complex, or the higher the bond strength between cation and hydroxyl anion. For a natural water with pH = 8, $[M^{+z}]/[M(OH)^{z-1}]$ ratios are greater than one, if the $\log {}^*K_1$ values of the cations are less than -8 according to equation I-5a (mostly mono- and divalent cations in Table I-11). Cations with $\log {}^*K_1 > -8$ are strongly to fully hydrolyzed (mostly tri- and tetravalent cations). Cations with valence equal to or greater than four often form oxyanions.

As one would have expected, $\log {}^*K_1$ and $\log {}^*k_i$ are linearly correlated with I_z and $z \cdot \chi_M^{+z}$ for cations, as shown in Figure I-21B ($\log {}^*k_i$ values are not shown here) and Figure I-21A, respectively. The obvious exceptions are Be^{+2} and again some of the heavy B-type cations, such as Tl^+, Ag^+, Hg^{+2}, Pb^{+2}, Tl^{+3}, and Bi^{+3}. The $\log {}^*K_1$ and $\log {}^*k_i$ values are also linearly correlated with the logarithm of the complexation constants of cations with a given organic ligand (Balistrieri et al., 1981). Figure I-22 (see page 51) shows the example of the EDTA ligand for a reaction of $M^{+z} + L^{-4} \rightarrow ML^{z-4}$. In other words, the larger the $\log {}^*K_1$, the higher the tendency for the cation in solution to form hydroxyl and metal–organic ligand complexes and the higher the bond strengths between the cation and a given anion or ligand.

TABLE I-11
First hydrolysis constants of cations at 25°C and $I = 0$

Z	z	$-\log {}^{*}K_1$	Z	z	$-\log {}^{*}K_1$	Z	z	$-\log {}^{*}K_1$
Ac-89	3	10.4	Hf-72	4	0.3S	PuO_2^{+2}	6	5.6
Ag-47	1	12	Hg-80	2	3.4	Rb-45	3	3.3C
Al-13	3	5	Ho-67	3	8	Ru-44	3	2.2R
Am-95	3	5.8S	In-49	3	4	RuO_4^0	8	11.9
Ba-56	2	13.5	Ir-77	3	4.4C	Sc-21	3	4.3
Be-4	2	5.4	K-19	1	14.5	Sm-62	3	7.9
Bi-83	3	1.1	La-57	3	8.5	Sn-50	4	−1.5
Bk-97	3	5.5S	Li-3	1	13.6	Sr-38	2	13.3
Ca-20	2	12.9	Lu-71	3	7.6	Tb-65	3	7.9
Cd-48	2	10.1	Mg-12	2	11.4	Th-90	4	3.2
Ce-58	3	8.3	Mn-25	2	10.6	Ti-22	3	2.2
	4	−0.7		3	−0.3	TiO^{+2}	4	2.3
Cf-98	3	5.5S	Na-11	1	14.2	Tl-81	1	13.2
Cm-96	3	5.8S	Nd-60	3	8		3	0.62
Co-27	2	9.7	Ni-28	2	9.9	Tm-69	3	7.7
	3	1.3	Np-93	4	1.5	U-92	4	0.65
Cr-24	3	4	NpO_2^+	5	8.9	UO_2^{+2}	6	5.8
Cu-29	2	7.9	OsO_4^0	8	12.1	V-23	3	2.3
Dy-66	3	8	Pa-91	4	−0.84	VO^{+2}	4	5.4
Er-68	3	7.9	PaO_2^+	5	4.5	Y-39	3	7.7
Eu-63	3	7.8	Pb-82	2	7.7	Yb-70	3	7.7
Fe-26	2	9.5	Pd-46	2	(2.3)A	Zn-30	2	9
	3	2.2	Pr-59	3	8.1	Zr-40	4	−0.1S
Ga-31	3	2.6	Pu-94	3	7			
Gd-64	3	8		4	0.5			

Source: Data are mainly from Baes and Mesmer (1981). Other data are from (C) Cotton and Wilkinson (1988), (R) Rard (1985), and (S) Smith and Martell (1976).

Note: A: Pd value is at 17°C and in 0.1 M $NaClO_4$.

The dissociation of the hydrogen ion from an oxyacid (H_mA) can be represented by

$$H_mA \rightarrow H_{m-1}A^- + H^+ \qquad (K_1),$$

$$* \; H_{m-1}A^- \rightarrow H_{m-2}A^{-2} + H^+ \qquad (K_2),$$

where A is an oxyanion; m the number of hydrogen atoms in the oxyacid; and K_1 and K_2 the first and second **acid dissociation constants**.

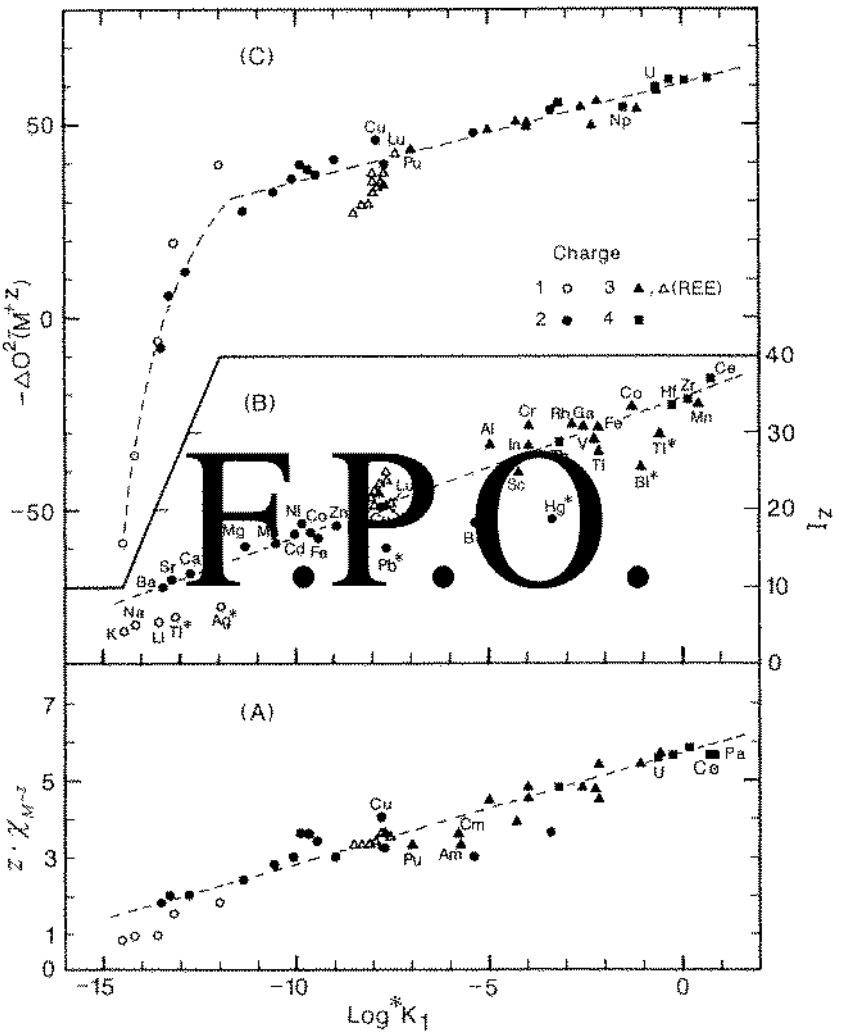

FIGURE I-21. Plots of $\log^* K_1$ (the first hydrolysis constant) versus (A) the total cationic electronegativity ($z \cdot \chi_{M^{+z}}$), (B) the electron binding energy I_z, and (C) the affinity of an aqueous cation to its oxide crystal ($-\Delta O^{2-}$). The ΔO^{2-} data are from Tardy and Garrels (1976).

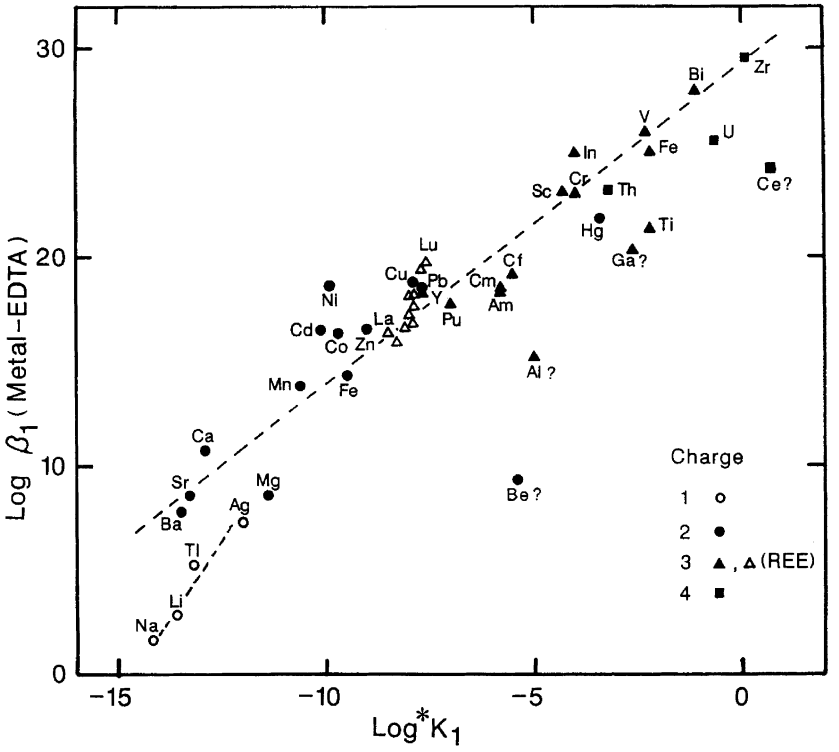

FIGURE I-22. Plot of $\log {}^{*}K_1$ (the first hydrolysis constant) versus $\log \beta_1^{\text{EDTA}}$ (the complexation constant of the cation to EDTA for the reaction $M^{+z} + L^{-4} \rightarrow ML^{z-4}$). The $\log \beta_1$ data are from Dean (1985) and Schwarzenback (1957).

The $\log K_1$ and $\log K_2$ values of various oxyacids are generally positively related to the I_z (or $z \cdot \chi_{M^{+z}}$) values of the central metals in the oxyacid as shown in Figure I-23 (only $\log K_1$ vs. I_z is shown). In other words, the higher the I_z (or $z \cdot \chi_{M^{+z}}$) value of the central metal in the oxyacid, the stronger the chemical bond strength between the central metal and the oxygen of the oxyanion, and the weaker the bond strength between the hydrogen ion and the oxygen of the oxyanion (i.e., strong acids). In general, the higher the $\log K_1$ and $\log K_2$ values are, the lower the tendency for the oxyanion to be adsorbed onto hydrous oxide particles. In short, the first hydrolysis constants of cations and dissociation constants of oxyacids are useful parameters to predict the affinity of cations and oxyanions to the surface of a hydrous oxide, aluminosilicate, or organic particles in aquatic environments. A detailed discussion is given in Chapter VI.

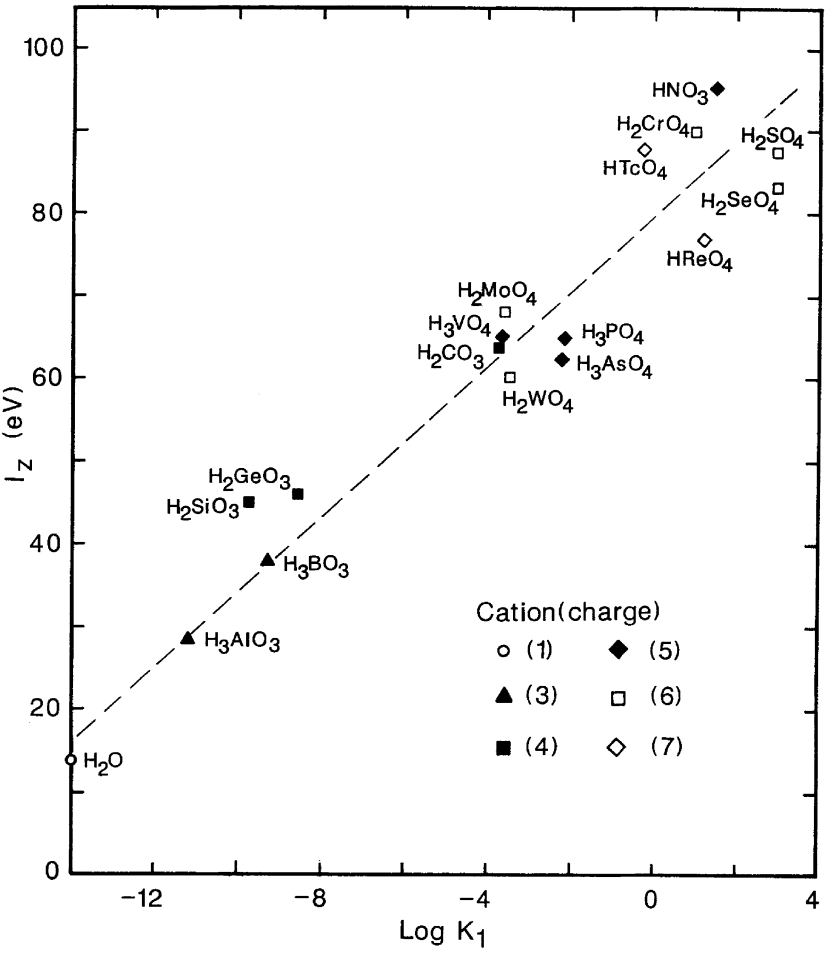

FIGURE I-23. $\log K_1$ (the first dissociation constant of an oxyacid) versus the I_z of the central metal in those oxyacids. The $\log K_1$ data are from Dean (1985).

I-10. SOLUBILITY PRODUCTS AND AFFINITY OF AQUEOUS CATIONS TO OXIDES

The precipitation or dissolution of metal oxides can be expressed by

$$\frac{1}{z}M^{+z} + \mathrm{OH}^- \leftrightarrow \frac{1}{2z} \cdot M_2O_z + \frac{1}{2}\mathrm{H_2O},$$

where K_{pt} is the forward reaction (precipitation) constant,

$$K_{pt} = \frac{1}{[M^{+z}]^{1/z}[OH^-]} = 10^{-\Delta\tilde{G}/(2.3RT)},$$

$\Delta\tilde{G}$ is the Gibbs free energy of the reaction, and K_{sp} is the solubility product,

$$K_{sp} = [M^{+z}][OH^-]^z$$
$$= 1/(K_{pt})^z.$$

Accordingly, $\log K_{pt}$ is equal to $-\log K_{sp}/z$ and proportional to $-\Delta\tilde{G} = \Delta G_f M^{+z}/z + \Delta G_f OH^- - \Delta G_f M_2O_z/2z - \Delta G_f H_2O/2$, or proportional to $(2\Delta G_f M^{+z} - \Delta G_f M_2O_z)/z$; thus these parameters are interchangeable. The higher these parameter values, the higher the tendency for the aqueous cation to form oxide precipitates, or the higher the average bond strength between cation and oxygen in an oxide crystal. We may call the parameter $(2\Delta G_f M^{+z} - \Delta G_f M_2O_z)/z$ the relative affinity of an aqueous cation to its oxide crystal, and it was designated as $-\Delta O^{2-}$ by Tardy and Garrels (1976). Therefore, $-\Delta O^{2-}$ is only another expression proportional to $-\log K_{sp}/z$.

The plot of $-\Delta O^{2-}$ (as well as $\log K_{pt}$ and $-\log K_{sp}/z$) versus $\log {}^*K_1$ shows again a roughly linear relationship (Figure I-21C). The obvious exceptions are alkali, alkaline earth, and some rare earth cations. One possible explanation is that the $\Delta\tilde{G}$ term contains not only the bond energy between cation and oxygen but also the cohesive energy for one mole of individual oxide molecules to aggregate into a solid crystal. As shown in Figures I-7 and I-8, ΔH^0_{sbl} values for alkali and alkaline earth metals are much lower than for other metals. Therefore, the oxide crystals of alkali and alkaline earth elements may also have much lower cohesive energies than other metal oxide crystals.

I-11. Concluding Remarks

The geochemical parameters discussed in this chapter are all closely interrelated quantities and all are in one way or another related to the concept of relative chemical bond strengths between cations and given ligands. The ionization energy data for various cations and anions are quite extensive and most are accurately determined. Therefore, the ionization energy or the electron binding energy, I_z, is one of the most useful geochemical parameters. I_z along with $\log {}^*K_1$ (first hydrolysis constant) and $\log K_1$ (first dissociation constant of oxyacids) are the most convenient overall parameters to relate the affinity of both cations and oxyanions to the surfaces of hydrous oxides, aluminosilicates, and organic particles in aquatic environments.

The total cationic electronegativities, $z \cdot \chi_{M^{+z}}$, are also linearly related to $\log {}^{*}K_1$ (Figure I-21) and to I_z (Figure I-17) except for some B-type and transition metal cations. Therefore the parameter $z \cdot \chi_{M^{+z}}$ should be as useful as the parameter I_z. The main drawbacks of the former are the larger uncertainty in determined values and somewhat limited data numbers.

The crystal lattice energies of oxides per oxygen ($\Delta H_L^0/n$) are essentially a linear function of both $\Sigma I_z/z$ and I_z (Figure I-20), and thus would not be more useful than the electron binding energies. The ionic potentials (z/r) of cations with a similar electron configuration are positively correlated to their I_z values (Figure I-14), but the ionic potential ignores the shielding effect of the electron sheath around the positively charged nucleus.

The classification of ions according to their electron configuration (A-type, B-type, etc.) and related parameters such as the electric polarizability (Table I-6) and the relative polarizability (Table I-7) is also a very useful tool to predict their chemical and geochemical behavior.